A Developmental Genetic Analysis of the Lysine Demethylase KDM2 Mutations in *Drosophila melanogaster*

Yani Zheng[*], **Fu-Ning Hsu**[*], **Wu Xu**[§], **Xiao-Jun Xie**[*], **Xinjie Ren**[†], **Xinsheng Gao**[*], **Jian-Quan Ni**[†], and **Jun-Yuan Ji**[*,1]

[*]Department of Molecular and Cellular Medicine, College of Medicine, Texas A&M University Health Science Center, College Station, TX 77843

[§]Department of Chemistry, University of Louisiana at Lafayette, P.O. Box 44370, Lafayette, LA 70504

[†]Gene Regulatory Laboratory, School of Medicine, Tsinghua University, Beijing 100084, China

Abstract

Post-translational modification of histones plays essential roles in the transcriptional regulation of genes in eukaryotes. Methylation on basic residues of histones is regulated by histone methyltransferases and histone demethylases, and misregulation of these enzymes has been linked to a range of diseases such as cancer. Histone lysine demethylase 2 (KDM2) family proteins have been shown to either promote or suppress tumorigenesis in different human malignancies. However, the roles and regulation of KDM2 in development are poorly understood, and the exact roles of KDM2 in regulating demethylation remain controversial. Since KDM2 proteins are highly conserved in multicellular animals, we analyzed the KDM2 ortholog in *Drosophila*. We have observed that dKDM2 is a nuclear protein and its level fluctuates during fly development. We generated three deficiency lines that disrupt the *dKdm2* locus, and together with 10 transposon insertion lines within the *dKdm2* locus, we characterized the developmental defects of these alleles. The alleles of *dKdm2* define three phenotypic classes, and the intragenic complementation observed among these alleles and our subsequent analyses suggest that dKDM2 is not required for viability. In addition, loss of dKDM2 appears to have rather weak effects on histone H3 lysine 36 and 4 methylation (H3K36me and H3K4me) in the third instar wandering larvae, and we observed no effect on methylation of H3K9me2, H3K27me2 and H3K27me3 in *dKdm2* mutants. Taken together, these genetic, molecular and biochemical analyses suggest that dKDM2 is not required for viability of flies, indicating that *dKdm2* is likely redundant with other histone lysine demethylases in regulating normal development in *Drosophila*.

[1]**Corresponding author:** Jun-Yuan Ji, Department of Molecular and Cellular Medicine, College of Medicine, Texas A&M University Health Science Center, Reynolds Medical Building, Room 233, College Station, TX 77843. ji@medicine.tamhsc.edu; Phone: (979) 845-6389.

Keywords

KDM2; histone H3; demethylase; development; *Drosophila*

Introduction

In eukaryotes, DNA wraps around core histones to form nucleosomes, which is compacted into high-order structures of chromosome in a highly dynamic and cell-cycle dependent manner. Covalent modifications of histone N-terminal tails, such as methylation, acetylation, and phosphorylation, correlate with chromatin structure and seem to influence multiple steps of transcription (Bannister and Kouzarides, 2011; Zentner and Henikoff, 2013). Accumulating evidences in recent years revealed that misregulation of these enzymes are linked to a range of diseases such as cancer (Chi et al., 2010; Greer and Shi, 2012; Timp and Feinberg, 2013).

Of variety of those post-translational modifications on histone tails, methylation of histone H3 Lysine 36 (H3K36me) shows a strong correlation with transcription elongation (Joshi and Struhl, 2005; Li et al., 2007; Smolle and Workman, 2013). Histone methyltransferase Set2 in yeast and nuclear receptor SET domain-containing 1 (NSD1) in humans control the methylation of H3K36 forming mono-, di- or tri-methylation on K36 (abbreviated as H3K36me1, H3K36me2 or H3K36me3, respectively) (Wagner and Carpenter, 2012). Conversely, the histone demethylases such as KDM2, KDM4 and KDM8 have been shown to specifically demethylate H3K36me (Crona et al., 2013; Hsia et al., 2010; Jones et al., 2010; Lin et al., 2012; Tsukada et al., 2006). There are two KDM2 paralogs in vertebrates: KDM2A (also known as FBXL11, JHDM1A, and Ndy2) and KDM2B (also known as FBXL10, JHDM1B, and Ndy1) (Allis et al., 2007; Cloos et al., 2008; Tsukada et al., 2006). Both proteins contain several conserved domains including the JmjC domain, a CXXC-type zinc finger, a PHD finger (Plant Homeo Domain), an F-box domain and several leucine-rich repeats (LRRs), and the JmjC domain harbors the demethylase activity (Blackledge et al., 2010; Cloos et al., 2008; Frescas et al., 2007; Lohse et al., 2011; Tsukada et al., 2006).

The importance of KDM2 is highlighted by studies that linking KDM2 to cancer development in recent years. However, the role of KDM2 seems to be either tumor suppressive or oncogenic, depending on specific types of cancers. On the one hand, KDM2 has been reported to function as a putative proto-oncogene in certain types of cancers. For example, the expression of *hKdm2b* gene is up-regulated in human leukemic stem cells and ectopic expression of hKDM2B is sufficient to transform hematopoietic progenitors (He et al., 2011). In addition, hKDM2B is required for *Hox9a/Meis1* -induced leukemic transformation, and hKDM2B regulates leukemic cell proliferation by directly repressing the expression of the tumor suppressor *Ink4b* (He et al., 2011). Similarly, depletion of KDM2B in primary mouse embryonic fibroblasts inhibits cell proliferation and induces senescence by direct depression of the *Ink4b* locus (He et al., 2008). Moreover, it was reported that KDM2B inhibits replicative or Ras-induced senescence by directly repressing the *Ink4a/Arf* locus in cultured mouse embryonic fibroblasts (Pfau et al., 2008; Tzatsos et al., 2009). KDM2B can also repress the expression of *c-Jun* (Koyama-Nasu et al., 2007). Furthermore,

KDM2B is found to be markedly overexpressed in pancreatic cancer cell lines and patient specimens, and its levels positively correlated to the severity of the disease (Tzatsos et al., 2013). Interestingly, mouse KDM2B is shown to be required for H2AK119 monoubiquitination and regulates mouse embryonic stem cell differentiation (Wu et al., 2013). Together with investigations on other KDMs, these studies have linked histone lysine demethylases to a variety of cancers, thus these enzymes have been considered as strong candidates for development of specific inhibitors in cancer therapy (Lohse et al., 2011; Rotili and Mai, 2011).

On the other hand, however, KDM2 has been reported to have tumor suppressive functions in other types of cancers. For instance, KDM2B inhibits cell growth and proliferation in HeLa cells (Frescas et al., 2007; Koyama-Nasu et al., 2007). Expression of KDM2B is significantly decreased in many primary brain tumors, and the decrease of KDM2B expression correlates with tumor grade (Frescas et al., 2007). In addition, retroviral disruption of KDM2B gene causes lymphoma in BLM-deficient mice (Suzuki et al., 2006). Furthermore, KDM2B binds to ribosomal DNA repeats and represses rRNA genes in nucleolus (Frescas et al., 2007). Consistent with this, hKDM2A is involved in repressing rDNA transcription in a demethylase activity-dependent manner in human breast cancer cells in response to starvation of glucose and serum (Tanaka et al., 2010). Compared to KDM2B, less is known about tumorigenic roles of KDM2A. It has been shown that KDM2A suppresses the growth of colon cancer cells by directly demethylating p65 (RelA) thereby inhibiting NF-κB activities (Lu et al., 2010). Taken together, these observations suggest a tumor suppressive role of KDM2. Considering the aforementioned oncogenic roles of KDM2 proteins, it thus appears that the role of KDM2 in cancer progression is dependent on specific biological contexts, which is consistent with the view that histone modification enzymes play context-specific roles in regulating tumorigenesis (Sarris et al., 2013).

Despite these studies, the role of KDM2s during development in the whole organisms remains poorly understood (Nottke et al., 2009). Simple model organisms such as *Drosophila* provide a plethora of genetic tools that can facilitate the studies of the evolutionarily conserved regulatory mechanisms *in vivo*. The *Drosophila* KDM2 (dKDM2) is the single homolog of the mammalian KDM2A and KDM2B (Fig. 1A) (Dui et al., 2012; Jin et al., 2004; Kavi and Birchler, 2009; Lagarou et al., 2008). Biochemical purification for dRING-associated proteins coupled with mass spectrometric analysis led to the identification of dKDM2 as a component of dRING-associated factors complex (dRAF), a Polycomb group (PcG) silencing complex composed of dRING, Posterior Sex Comb (PSC) and dKDM2 (Lagarou et al., 2008). Depletion of dKDM2 in cultured S2 cells significantly increased levels of H3K36me2 and caused loss of H2A ubiquitination, but did not affect the levels of H3K36me1, H3K36me3 and H3K4me3 (Lagarou et al., 2008). These observations demonstrate that dKDM2 plays a key role in dRAF complex by mediating both demethylation of H3K36me2 and ubiquitination of H2A (Lagarou et al., 2008). Similar approach using murine erythroleukemia cells led to the identification of KDM2B as a component of the KDM2B-RING1B complex, which includes RING1B, Bcl6 corepressor (BCoR), Skp1, and a few other proteins that are involved in regulating H2A ubiquitination (Sanchez et al., 2007). Depletion of KDM2B was also shown to significantly reduce H2A

ubiquitination in mouse embryonic stem cells (Wu et al., 2013). However, knocking down dKDM2 *in vivo* using *actin5C-Gal4* to drive the expression of *dKdm2-dsRNA* in the third instar larvae did not reveal any effects of dKDM2 depletion on the levels of H3K36me2, H3K9me2, and H3K4me2 assayed by Western blot and immunofluoresence staining; instead, a strong increase of H3K4me3 was observed, suggesting that dKDM2 specifically demethylates H3K4me3 *in vivo* (Kavi and Birchler, 2009). In addition, depletion of dKDM2 in salivary glands resulted in multiple nucleoli (Kavi and Birchler, 2009). These observations are consistent to the role of KDM2B in repressing rRNA gene expression by demethylating H3K4me3 in nucleolus (Frescas et al., 2007). It is still unclear why dKDM2 displayed different functions in these two reports. Perhaps, dKDM2 can serve as a component in multiple protein complexes that regulate different target genes, thereby enabling it to demethylate H3K4me3, or H3K36me2, or both, in a context-specific manner.

To clarify the functions of dKDM2 *in vivo*, it is essential to analyze the loss of *dKdm2* mutants during development. No studies performed to date, however, have characterized the phenotypes of *dKdm2* mutants, because no null alleles of *dKdm2* are available and several *dKdm2* alleles caused by transposon insertions remain uncharacterized. In this study, we analyzed the role of dKDM2 in *Drosophila* development by charactering the developmental defects of multiple *dKdm2* alleles and their effects on histone modifications *in vivo*. Specifically, we have generated three deficiency lines that remove the *dKdm2* locus, and then characterized these three deficiency lines together with 10 transposon insertion lines within the *dKdm2* locus. We observed that dKDM2 is a nuclear protein and is expressed throughout development with relatively low expression during the first and second larval stages. In addition, the effects of loss of dKDM2 on histone lysine 4 and lysine 36 methylation seem to be rather mild during the third instar wandering stage. Our genetic and biochemical analyses suggest that dKDM2 is not required for viability, indicating that the role of dKDM2 may be redundant with other histone demethylases.

Materials & Methods

Phylogenetic analysis

The amino acid sequences of KDM2 proteins from different species were downloaded from the National Center for Biotechnology Information (NCBI) database and imported to MEGA5 (Tamura et al., 2011). The pairwise algorithm and the Neighbor-Joining algorithm built in MEGA 5 were used to construct the phylogenetic tree. The NCBI Reference Sequence numbers for these KMD2 proteins are listed in Fig. S1, and the protein-protein BLAST (BLASTp) (Altschul et al., 1997) was used to search for the putative conserved domains for each KDM2 proteins (Fig. S1).

Fly Strains

Drosophila strains and crosses were maintained on standard cornmeal-yeast agar food at 25°C. We used w^{1118} flies as the control. The following *dKdm2* alleles were obtained from the Bloomington *Drosophila* Stock Center: $dKdm2^{DG12810}$ (genotype: $P[wHy]dKdm2^{DG12810}$), $dKdm2^{F11.1}$ (w^*; $P[ID.GAL4DBD]dKdm2^{F11.1}$), $dKdm2^{KG04325}$ ($y^1 w^{67c23}$; $P[SUPor-P]dKdm2^{KG04325} ry^{506}$), $dKdm2^{EY01336}$ ($y^1 w^{67c23}$;

$P[EPgy2]dKdm2^{EY01336}$), $dKdm2^{EP3093}$ (w^{1118}; $P[EP]dKdm2^{EP3093}/TM6B$, Tb^1). In addition, several P-element and PiggyBac insertion lines that were generated by Exelixis, including *d06162* (*P[XP]dKdm2^{d06162}*), *f02828* (*PBac[WH]dKdm2^{f02828}*), *d06730* (*P[XP]dKdm2^{d06730}*), and *e01422* (*PBac[RB]Ada^{e01422}*), were obtained from the Exelixis Collection at the Harvard Medical School (https://drosophila.med.harvard.edu/)

PCR analysis of the deletion lines

To prepare genomic DNAs (gDNAs) from the homozygous *Df(3R)J15* (first instar and the third instar larvae), *Df(3R)J16* and *Df(3R)J18* (third instar at the wandering stage) mutant larvae, we used the methods as described previously (Parks et al., 2004). First, we used the genomic PCR approach (Fig. 3A) with Taq polymerase (Invitrogen) for 35 elongation (5.0 min) and annealing (at 55°C) cycles. The following primers were used for Fig. 3B: 1F: 5'-CGAATATACGTGGAGCGTGA; 2R: 5'-TGGGGGTACTTGAAAATTCG; 3F: 5'-CGGTTGTAGCCGTTAGGAAA; and 4R: 5'-CTCGTGCACAAATGCAAACT. In addition, we used the hybrid PCR approach (Fig. 3D) to validate *Df(3R)J15* and *Df(3R)J15#* lines using primers F: 5'-ATGATTCGCAGTGGAAGGCT and R: 5'-GACGCATGATTATCTTTTACGTGAC; for *Df(3R)J16* and *Df(3R)J18* lines, we used these primers: F: 5'-ATGATTCGCAGTGGAAGGCT and R: 5'-TGCATTTGCCTTTCGCCTTAT. The w^{1118} line was used as the control for these reactions.

Validation of the transposon insertion lines by PCR

Similarly, the insertion alleles of *dKdm2* were also validated by PCR using the gDNA of each allele. We used Taq polymerase (Invitrogen) with 3.5 min as elongation time to ensure all the fragments (<2.7kb) can be amplified and the annealing temperature was 55°C. The primers used for the positive control reaction are: "*dKdm2-34F*" 5'-AATCTTCAAAGTTCGCGCAGG and "*dKdm2-56R*" (5'-GCAATGTATTTCCATCCGCG-3'), which generate a 2682-bp product (Fig. S3). The primers for specific alleles are listed below: for *dKdm2^{d00170}* allele (F: 5'-ATAGGTTGTGGAAGCGAACG; R: 5'-ACGCCCACGTATCACTTTTC), *dKdm2^{DG12810}* allele (F: 5'-GCGGAAAGGCATAATTGAAA; R: 5'-TCGCCTTCACTTTCTCCAGT), *dKdm2^{EY01336}* allele (F: 5'-GCGGCCAAAATAAACTCAAA; R: 5'-GCCTTCACTTTCTCCAGTCG), *dKdm2^{F11.1}* allele (F: 5'-GCGGCCAAAATAAACTCAAA; R: 5'-GCCTTCACTTTCTCCAGTCG), *dKdm2^{KG04325}* allele (F: 5'-ATAGGTTGTGGAAGCGAACG; R: 5'-ACGCCCACGTATCACTTTTC), *dKdm2^{EP3093}* allele (using the gDNA from *dKdm2^{EP3093}/TM6B* as the template, the following two set of primers were used: F1: 5'-TGGAATCGACCTTTCTTTGC; R1: 5'-CGGGATATGGAGCAGTTGTT; F2: 5'-TGGAATCGACCTTTCTTTGC; R2: 5'-CGGGATATGGAGCAGTTGTT). The same primers were used to verify the background cleaned-up *dKdm2^{d00170#}*, and *dKdm2^{EP3093#}* alleles. The primers used to verify the *dKdm2^{f02828#}* allele are F: 5'-GCGGCCAAAATAAACTCAAA and R: 5'-GCCTTCACTTTCTCCAGTCG. Taq DNA polymerase (Invitrogen) was used in the PCR reactions, the annealing temperature was 55°C, and the elongation time was 3.5 min to ensure all the fragments (<2.7kb) can be amplified.

qRT-PCR analysis

We performed qRT-PCR analyses using the StepOnePlus Real-Time PCR System (Applied Biosystems) as previously described (Zhao et al., 2012). The qPCR primers were designed using Primer Express software (Applied Biosystems), and the following primers were used to detect the mRNA levels of *dKdm2* and three of its neighboring genes (*Mst85C*, *beag* and *ada*) during the larval stage: *dKdm2-23* (F: 5'-GTCCAAATGCAAAAGGCGTG; R: 5'-AGATTCGAGCTTCTCGGCAAC), *dKdm2-34* (F: 5'-AATCTTCAAAGTTCGCGCAGG; R: 5'-CGCTTTGTCCCGGAATAACAG), *dKdm2-56* (F: 5'-CCGCTCTGGCAAAAACTATGAC; R: 5'- GCAATGTATTTCCATCCGCG), *Mst85C* (F: 5'-GCATAAGCGAAAATCCGAGCA; R: 5'-TCTTCGGATCCAGCGATAGACC), *beag* (F: 5'-GTCCTTTGGCAGTTTTCGCTT; R: 5'-ACTACATGAGCACGAAGGAGGC), *ada* (F: 5'-GCGATTCGAGATTTCGCTGA; R: 5'-TCACGATCTGCAGGTAGTCCCT), and *rp49* (F: 5'-ACAGGCCCAAGATCGTGAAGA; R: 5'-CGCACTCTGTTGTCGATACCCT) was used as the reference gene. Since hKDM2B was reported to repress rRNA gene expression and knocking down of dKDM2 in salivary glands leads to multiple nucleoli (Frescas et al., 2007; Kavi and Birchler, 2009), we verified the levels of *Rp49* gene using *GAPDH* and found no effect of *dKdm2* on the levels of *Rp49* gene (data not shown). The quality of the qRT-PCR primers was verified by examining the melting curve and electrophoresis in 1.2% agarose gel. In all cases, three independent biological repeats of each genotype were assays.

Generation of GST-dKDM2 fragments

To generate the GST-fused dKDM2 (AA1~220) protein, we used the Gateway Technology (Invitrogen). Briefly, AA1~220 was amplified using Phusion High-Fidelity DNA Polymerases (F-530S; New England Biolabs) and following primers: F: 5'-CACCATGTCCACCGCCGTTGAAACG and R: 5'-TCATAGCAGATTGGTGCCCTCCCG. The annealing temperature for the PCR reaction was 60°C and elongation time was 2.0 min for 35 cycles. The PCR product was purified, then ligated into the pENTR/D-TOPO vector using the pENTR/D-TOPO Cloning kit (K240020, Invitrogen), and subsequently verified by sequencing. The pDEST15 was used as the destination vector and the *att* L × *att* R reaction was mediated by LR Clonase II enzyme mix (11791-020, Invitrogen) following the manufacturer's protocols. The GST-fused dKDM2 (AA1~220; Fig. S2) was expression of pDEST15-dKDM2 (AA1~220) in *E. coli* (Rosetta) cells. The GST-fusion protein was purified and stained with the Commassie blue following the standard biochemical methods.

Western blot analysis and antibodies

Polyclonal rabbit antiserum against dKDM2 was generated using peptide AA37~56 (KGVQRRQLRERKQRKKYLEE) as the antigen. The rabbit immunizations were performed by Pierce Biotechnology, Thermo Scientific (Rockford, IL). The antiserum was purified using GST-fused dKDM2 (AA1~220; Fig. S2) using the protocol as described previously (Tang, 1993). Cytoplasmic, nuclear soluble, and nuclear insoluble fractions of protein extractions were prepared following the protocol as described (Lin et al., 2012). We

found that dKDM2 is only present in the nuclear soluble fraction (Fig. 2), thus the levels of dKDM2 in this fraction were further analyzed in all of the subsequent experiments.

To analyze histone modification, we prepared histones from the third instar larvae at the wandering stage or cultured *Drosophila* S2-DRSC cells using the EpiSeeker Histone Extraction Kit (ab113476 from Abcam, Cambridge, UK). Briefly, 15 larvae per sample, three samples per genotype, were grinded in 300 μl 1X Pre-lysis Buffer, centrifuge at 1,000 rpm at 4° for 1.0 min and the pellet was re-suspended in 100 μl of Lysis Buffer. The rest of the steps were performed according the manufacture instructions. The experiments were repeated several times and the representative results are presented. Antibodies against histone modifications include: antihistone H3 (9717S; 1:2000), anti-H3K4me2 (9725; 1:2000) were from Cell Signaling Technology (Danvers, MA); while anti-H3K4me1 (ab8895; 1:2000), anti-H3K4me3 (ab8580; 1:2000), anti-H3K9me2 (ab1220; 1:2000), anti-H3K27me2 (ab24684; 1:2000), anti-H3K36me1 (ab9048; 1:2000), anti-H3K36me2 (ab9049; 1:2000), and anti-H3K36me3 (ab9050; 1:2000) were purchased from Abcam, and anti-H3K27me3 (07-447; 1:2000) was from Millipore (Temecular, CA). The Actin pan monoclonal antibody (MA5-11869, 1:4000) was purchased from Thermo Scientific (Waltham, MA).

Generation of *dKdm2*-dsRNAs and depletion of dKDM2 in S2-DRSC cells

To avoid potential off-target effects, the dsRNAs targeting *dKdm2* and *white* were designed using the online program developed by Dr. Norbert Perrimon lab (http://www.flyrnai.org/cgi-bin/RNAi_find_primers.pl). The dsRNAs were generated following the same protocols as described previously (Dimova et al., 2003; Ji et al., 2012). The following primer sets were used to generate dsRNAs to *dKdm2-1* (F: 5'- GTTCTCTCTGGCAAACAGGC; R: 5'-TACCTCTGCATTCTTGCGTG), *dKdm2-2* (F: 5'- GGACACGCTGGTTACCTGTT; R: 5'-ATAACCACACGCAATGCAAA). The PCR reactions were performed using the *dKdm2* cDNA as the template. The PCR products were purified, sub-cloned into pGEM-T vector (Promega), and verified by sequencing. The primers with T7 sequences are following: *T7-dKdm2-1* (F: 5'-CTAATACGACTCACTATAGGGAGGTTCTCTCTGG; R: 5'-CTAATACGACTCACTATAGGGAGTACCTCTGCATTC), *T7-dKdm2-2* (F: 5'-CTAATACGACTCACTATAGGGAGGGACACGCTGG; R: 5'-CTAATACGACTCACTATAGGGAGATAACCACACGC). The S2-DRSC cell line was obtained from the *Drosophila* Genomics Resource Center (Bloomington, IN). As verified by Western blot, both *dKdm2* -dsRNAs effectively depleted dKDM2 proteins in S2-DRSC cells after 4 days of treatment.

Results

Characterization of the conserved protein domains in KDM2 homologs

KDM2 is conserved in yeast and multicellular animals, especially in the JmjC domain (Tsukada et al., 2006). Interestingly, KDM2 is not present in plants (Zhou and Ma, 2008). There are two KDM2 paralogs in vertebrates and one KDM2 homolog in invertebrates (Fig. 1A). Although the amino-acid sequence and domain structures of KDM2 proteins are not completely conserved from yeasts to humans, they share the JmjC domain, a CXXC Zinc

finger, an F-box domain, and an Amn1 (Antagonist of mitotic exit network protein 1) domain that usually overlaps with leucine-rich repeats (LRRs) (Cloos et al., 2008; Dui et al., 2012; Jin et al., 2004; Tsukada et al., 2006).

To portray the evolutionary history of these different domains of KDM2, we built a phylogenetic tree of KDM2 proteins in a few representative multicellular animals. The KDM2 proteins from *C. elegans* to humans share the JmjC domain, which encodes the histone demethylase motif (Fig. 1A and Fig. S1). However, the *C. elegans* KDM2 lacks all other domains found in KDM2. Interestingly, the PHD finger can be found in vertebrates and vase tunicate (*Ciona intestinalis*), a urochordate (sea squirt), but it is not present in purple sea urchin (*Strongylocentrotus purpuratus*), which belongs to Echinodermata, and other invertebrates (Fig. 1A). In addition, although a KDM2A-like protein was annotated in purple sea urchin, this KDM2A-like protein only share the similarity in its CXXC zinc finger with other KDM2 proteins (Fig. 1A), suggesting that the sea urchin KDM2B-like protein is likely the only KDM2 protein that has demethylase activity. Therefore, besides JmjC domain, the CXXC zinc finger, F-box and LRRs/Amn1 domains are highly conserved in KDM2 proteins.

Unlike vertebrates, *Drosophila* contains only one ortholog of KDM2, encoded by *CG11033* or *dKdm2* gene (Kavi and Birchler, 2009; Lagarou et al., 2008). As shown in Fig. 1B, except the least conserved PHD finger, dKDM2 contains all the other conserved domains, including JmjC, CXXC zinc finger, F-box and the Amn1/LRRs domains. These features make *Drosophila* an attractive experimental system to genetically dissect the function and regulation of KDM2 during development.

Expression of dKDM2 during *Drosophila* development

To study the role of KDM2 in development, we characterized the expression of *dKdm2* during developmental stages by quantitative reverse transcriptase PCR (qRT-PCR) assay. Based on the high throughput sequencing analysis (Graveley et al., 2011), *dKdm2* locus encodes 4 transcripts that only differ in their exon 1 that encodes part of the 5' untranslated region (5' UTR). Each isoform of *dKdm2* transcript contains six exons separated by five introns (Fig. 2A). The exon 1 and part of exon 2 encode the 5' UTR, while part of exon 6 encodes the 3' UTR (Fig. 2A). Because *dKdm2* gene contains six exons that span ~ 11 kb of genomic DNA, we designed three pairs of primers that span three exon-exon junctions of the *dKdm2* gene: "*dKdm2-23* " spans the exon 2 and exon 3, "*dKdm2-34* " spans the exon 3 and exon 4, and "*dKdm2-56* " spans the exon 5 and exon 6 (Fig. 2A). As shown in Fig. 2B, high levels of *dKdm2* mRNA were detected during the embryonic, third instar larval, pupal stages, as well as in adult flies.

To analyze dKDM2 protein, we first generated a polyclonal rabbit antibody using a peptide (AA 37~56) of dKDM2 as the antigen (see Materials and Methods). We then purified the antiserum using AA1~220 of dKDM2 fused with GST (Fig. S2: Coomassie blue staining), which can be recognized by the polyclonal antibody (Fig. S2). We further validated the specificity of this antibody using the null mutants of *dKdm2* (see below in Fig. 4H) and cultured S2-DRSC cells with dKDM2 depleted (Fig. 4G). With this purified antibody, we analyzed the subcellular localization of dKDM2 by separating proteins in the cytosol,

nuclear soluble and nuclear insoluble fractions from the third instar larvae, since this polyclonal antibody did not work with immunostaining. We observed that dKDM2 is a little bit over 150 kDa on the immunoblot after SDS-PAGE (Fig. 2C and Fig. 2F), while dKDM2 is predicted to be 146.2 kDa considering composing of 1,345 AA, presumably due to post-translational modifications. Importantly, dKDM2 is only present in the nuclear soluble fraction from the wild type but not the mutant larvae (Fig. 2C and see below). In addition, dKDM2 is not present in the cytosolic and nuclear insoluble fractions (Fig. 2D and 2E), suggesting that dKDM2 is a nuclear protein.

Next, we analyzed the levels of nuclear dKDM2 in different developmental stages. As shown in Fig. 2F, the levels of dKDM2 protein is high in embryos, but it is almost undetectable in the first and second instar larvae, and subsequently it reappears during the third instar, pupal and adult stages. This pattern of the dKDM2 protein is similar to its mRNA profile during development (Fig. 2B), suggesting that dKDM2 may function during embryogenesis and in biological processes after the third instar larvae.

Generation and characterization of the chromosomal deletions around the *dKdm2* locus

To understand the function and regulation of dKDM2 during development, it is essential to analyze the phenotypic consequences when *dKdm2* is mutated. Since no null allele of *dKdm2* was available, we generated three deficiency lines in *dKdm2* locus using the FLP-FRT deletion approach (Parks et al., 2004). This method takes the advantage of the large collection of isogenic *piggyBa* c and *P*-element insertion lines that contain FRT sites (Thibault et al., 2004), expression of flipase recombinase in transheterozygous of two insertions flanking a genomic region of interest efficiently removes the genomic region with precisely defined endpoints (Parks et al., 2004). The *dKdm2* gene is ~11kb long and localized in cytogenetic region 85C3-85C4 of third chromosome (Fig. 3A). To delete the *dKdm2* gene, we used several *piggyBac* (*f02828* and *e01422*) and P-element (*d06162* and *d06730*) insertion lines inside of or flanking the *dKdm2* locus (Fig. 3A). After verification and confirmation of the reported insertion sites and orientation of these lines (data not shown), we generated three deletion lines, designated as "*Df(3R)J15* ", "*Df(3R)J16* ", and "*Df(3R)J18* " (Fig. 3A). Of these deletions, *Df(3R)J15* removes ~3.6kb of the *dKdm2* gene between *d06162* and *f02828*, while *Df(3R)J16* deletes ~12kb of the genomic region between *d06162* and *e01422*, which includes *dKdm2* and its neighboring gene *beag* (*CG18005* at 85C4, Fig. 3A). Since the endpoint of *Df(3R)J16* is very close to gene *Ada* (*CG11994* at 85C4, encodes the Adenosine deaminase), this deletion may also affect the expression of *Ada* (see below). Similarly, *Df(3R)J18* is smaller than *Df(3R)J16*, it deletes the ~7.5kb region between *d06730* and *e01422*, including both *dKdm2* and *beag* (Fig. 3A).

We used two methods for the PCR verification of deficiency lines in heterozygous adult flies (*Df(3R)J15/TM6B Tb*, *Df(3R)J16/TM6B Tb*, and *Df(3R)J18/TM6B Tb*). First, we performed genomic PCR using primers flanking the deleted regions (Fig. 3A). Short elongation time was set so that only the deletions with the short leftover of transposons (<5kb) were amplified. As shown in Fig. 3B, a PCR fragment of expectation size was amplified in the deficiency lines (*Df(3R)J15/TM6B Tb*, *Df(3R)J16/TM6B Tb and Df(3R)J18/TM6B Tb*), while no PCR product amplified in control (w^{1118}) when using primers for

Df(3R)J16/TM6B Tb and *Df(3R)J18/TM6B Tb*. Second, we used the hybrid PCR method to amplify the hybrid leftovers of the two transposons after recombination (Fig. 3C) (Parks et al., 2004). As shown in Fig. 3D, the transposon leftover PCR products were amplified in these deficiency lines but not in the control, suggesting that these deletions are located in the expected genomic regions. In addition, to precisely map the breakpoints of these deficiency lines, we sequenced the PCR products from the genomic PCR (Fig. 3B). We found that *Df(3R)J15* deleted the region 4878938 ~ 4882546 of the third chromosome, *Df(3R)J16* deleted the region 4878938 ~ 4890949, while *Df(3R)J18* deleted the region 4883430 ~ 4890949, which are exactly as what we expected from the insertion sites.

Taken together, these analyses demonstrate that *Df(3R)J15* removes part of the *dKdm2* gene, while *Df(3R)J16* and *Df(3R)J18* delete both *dKdm2* and its neighboring gene *beag* (Fig. 3A). Interestingly, the homozygous mutants of *Df(3R)J15* are completely lethal during the first instar, while the homozygous mutants of *Df(3R)J16* and *Df(3R)J18* develop slower but are lethal during third instar larval and pupal stage. This appears puzzling considering that *Df(3R)J16* and *Df(3R)J18* are larger deletions than *Df(3R)J15* (Fig. 3A), thus we further analyzed these deletion lines together with additional *dKdm2* alleles described below.

Characterization of additional *dKdm2* alleles caused by insertions of transposable elements

Analyzing multiple alleles of the gene of interest is essential to reveal the spectrum of its function during development. While generating and analyzing the deletion lines, several transposon insertion lines within the *dKdm2* locus were made available from the Bloomington *Drosophila* Stock Center. These include *dKdm2^{EP3093}* (*P[EP]dKdm2^{EP3093}*), *dKdm2^{KG04325}* (*P[SUPor-P]dKdm2^{KG04325}*), *dKdm2^{DG12810}* (*P[wHy]dKdm2^{DG12810}*), *dKdm2^{EY01336}* (*P[EPgy2]dKdm2^{EY01336}*), and *dKdm2$^{F11.1}$* (*P[ID.GAL4DBD]dKdm2$^{F11.1}$*) (Bellen et al., 2004; Gohl et al., 2011; Huet et al., 2002; Myrick, 2005) (Fig. S3A). Although the insertion sites for some of these lines have been vetted by high throughput methods, no developmental genetic analyses of these alleles have been reported to date. In addition, the phenotypic consequences of these mutants differ from each other and from the deficiency lines that we generated. Therefore, it is important to validate these mutant alleles before any further analysis.

To verify the insertion sites, we performed PCR assays using the genomic DNA of these alleles as the templates. For *dKdm2^{EY01336}* allele, we used the two-sided PCR strategy (Fig. S3B, (Parks et al., 2004)) and confirmed the presence of the insertion (Fig. S3C). For the rest of the insertion lines, we used the genomic PCR approach (Fig. S3D). Insertions of 10-15kb transposons will not allow the amplification of the gDNA fragments between 600bp and 1.5kb, and our results confirmed all these alleles (Fig. 3E). In addition, we also validated five insertion lines generated by Exelixis (Thibault et al., 2004), including one piggyBac (*PBac[WH]dKdm2^{f02828}*) and four P-element (*P[XP]dKdm2^{d00170}*, *P[XP]dKdm2^{d02926}*, *P[XP]dKdm2^{d06162}*, and *P[XP]dKdm2^{d06730}*) insertion lines (Fig. 3A, Fig. S3A, and data not shown). Taken together, these results confirmed the reported insertion sites of these insertion lines.

Next, we analyzed homozygous mutants of these 10 insertion lines. As summarized in Table 1, we observed that the homozygous $dKdm2^{EP3093}$ mutants are lethal during the first instar; the $dKdm2^{d00170}$ mutants are lethal during late third instar, while the $dKdm2^{DG12810}$ mutants are lethal at the pupal stage. However, the homozygous of all the other seven insertion lines are fully viable (Table 1).

Based on the lethal phase of the homozygous mutant animals, we classified all the 13 available $dKdm2$ alleles into three classes (Table 1). The homozygous mutants of the class I alleles, including $Df(3R)J15$, $dKdm2^{EP3093}$, and $dKdm2^{f02828}$, are lethal during the first instar larval stage (L1). The homozygous mutants of the class II $dKdm2$ alleles develop slower, and all of them are lethal during the third instar larval (L3) stage, or pupal (P) stage, or both (Table 1). The class II alleles include $Df(3R)J16$, $Df(3R)J18$, $dKdm2^{d00170}$, and $dKdm2^{DG12810}$. In contrast to these two classes, the mutant animals of the class III $dKdm2$ alleles, including $dKdm2^{d02926}$, $dKdm2^{d06162}$, $dKdm2^{d06730}$, $dKdm2^{EY01336}$, and $dKdm2^{F11.1}$, and $dKdm2^{KG04325}$, are fully viable and fertile, and we did not observe any developmental defects with these homozygous mutants (Table 1).

Complementation tests of the multiple *dKdm2* alleles

Because homozygous mutants of multiple alleles of $dKdm2$ are either fully viable or lethal during larval and pupal stages, we performed complementation test and analyzed the viability of transheterozygous combinations of any of two $dKdm2$ alleles. As summarized in Table 1, we found that transheterozygous combination of $dKdm2^{f02828}$ and $Df(3R)J15$ (genotype: $w^{1118}; +; dKdm2^{f02828}/Df(3R)J15$) are lethal during L1 stage, similar to homozygous mutants of either $dKdm2^{f02828}$ or $Df(3R)J15$. Since $Df(3R)J15$ was generated by removing the genomic regions between $dKdm2^{f02828}$ and $dKdm2^{f06162}$, these two lines share similar genetic background and they are further analyzed below. In addition, we observed that transheterozygous combination of $Df(3R)J16$ and $Df(3R)J18$ (genotype: $w^{1118}; +; Df(3R)J16/Df(3R)J18$) are lethal during L3 and pupal stage, similar to homozygous mutants of either $Df(3R)J16$ or $Df(3R)J18$ alone (Table 1). Other than these two exceptions, however, all of the transheterozygous combinations of other $dKdm2$ alleles are fully viable, fertile, and showed no developmental delays (Table 1). In fact, the transheterozygous combinations of $dKdm2$ alleles can be maintained as stocks for generations (data not shown), indicating that dKDM2 is not essential for normal development of both somatic and germline cells, which will be further analyzed below.

Effects of *dKdm2* alleles on the expression of *dKdm2* and its neighboring genes

If $dKdm2$ is not required for normal development, why are the class I and class II alleles of $dKdm2$ lethal during the larval and pupal stages? One possibility to explain why the transheterozygous animals among class I and class II $dKdm2$ alleles are fully viable is that the expression of $dKdm2$ is normalized when these alleles were paired in trans, possibility through mechanisms such as transvection, or paring-dependent intragenic complementation (Kennison and Southworth, 2002; Wu and Morris, 1999). Several mechanisms have been proposed to explain the heteroallelic complementation, including trans-acting regulatory RNAs, transsplicing of RNAs, and trans-acting enhancer element (Kennison and Southworth, 2002; Wu and Morris, 1999). This hypothesis predicts that the expression of

dKDM2 is normalized when two defective alleles are supplied in trans. Alternatively, dKDM2 is not required for normal development and the lethality of certain alleles are caused by potential second-site mutation(s) in the genetic backgrounds, which would have opposite prediction on *dKdm2* mRNA and protein levels.

To distinguish these two scenarios, we analyzed the mRNA and protein levels of *dKdm2* in both homozygous and trans-heterozygous mutants. First, we analyzed the effects of class I and class II *dKdm2* alleles on the expression of *dKdm2* and its neighboring genes, including *Mst85C*, *beag* and *Ada*, by qRT-PCR assay, since these neighboring genes may also be affected in some alleles. Fig. 4A shows the schematic view of the *dKdm2* locus with its neighboring gene and the relative position of the qPCR primers used in this analysis. Three pairs of primers spanning the exons of *dKdm2* locus allowed us to exclude amplification from genomic DNA contamination, but also assay the effect of transposon insertions within the introns on mRNA expression (Fig. 4A). We focused our analysis on homozygous mutants of the one class I *Kdm2* alleles (*Df(3R)J15*), four class II *dKdm2* alleles, including *Df(3R)J16*, *Df(3R)J18*, *dKdm2^{d00170}*, and *dKdm2^{DG12810}*, as well as a few class III *dKdm2* alleles.

For class I allele *Df(3R)J15*, we analyzed the homozygous mutants in L1 stage since they are lethal in this stage. We could not detect *dKdm2* mRNA with the qPCR primers that span the exon 2 and exon 3 of the *dKdm2* gene in *Df(3R)J15* homozygous mutants (Fig. 4B), which is consistent to the complete deletion of exon 2 in *Df(3R)J15* allele. Surprisingly, however, qPCR primers that monitor exon 3 to exon 6 revealed a 4~8 fold increase (Fig. 4B), suggesting that a truncated dKDM2 protein may be ectopically expressed in the *Df(3R)J15* mutants. We note that the antigen used to generate the polyclonal antibody (AA37~56) spans the deleted first exon, preventing us from detecting an overexpressing of the truncated dKDM2.

For class II alleles, we examined the gene expression in the homozygous mutants at the wandering (late third instar) stage. We observed that both *dKdm2* and *beag* are not detectable in both *Df(3R)J16* (Fig. 4C) and *Df(3R)J18* (Fig. 4D) mutant larvae, while *Mst85C* is not affected by these deletions. Unexpectedly, however, the expression of *Ada* is increased 2~5 folds in these two deletions (Fig. 4C and Fig. 4D). Perhaps, deletion of *beag* and most part of *dKdm2* allows the residual regulatory elements of *dKdm2* to drive the aberrant expression of *Ada* (Table 1). Since *Df(3R)J15* and *Df(3R)J16* share the same breakpoint within the first intron of *dKdm2* locus, our observation of upregulation of exons 2-5 of *dKdm2* in *Df(3R)J15* (Fig. 4B) and ectopic expression of *Ada i* n *Df(3R)J16* (Fig. 4C) suggests that transcription of *dKdm2* may be controlled by regulatory elements within the first intron or further upstream of the transcription start site. Similarly, we analyzed *dKdm2^{d00170}* homozygous mutants and found that *dKdm2* mRNA is significantly reduced when detected with three sets of *dKdm2* primers, but its neighboring genes *Mst85C* and *beag* are also reduced (Fig. 4E). Furthermore, we analyzed *dKdm2^{DG12810}* homozygous mutants and observed that *dKdm2* mRNA is significantly reduced compared to the control, and the expression of the *dKdm2* neighboring genes was not affected (Fig. 4F).

Besides the mRNA levels of *dKdm2* gene, we also analyzed the effects of these *dKdm2* alleles on dKDM2 protein levels by Western blot. Since the levels of dKDM2 protein are high during embryonic, third instar larval, pupal and adult stages (Fig. 2F), we analyzed the class II *dKdm2* homozygous mutants during the third instar stage and found that dKDM2 was undetectable in *Df(3R)J16* and *dKdm2^{DG12810}* homozygous mutants (Fig. 4G and Fig. 4H). Similar to *Df(3R)J16* and *dKdm2^{DG12810}* homozygous mutants, dKDM2 was also undetectable in *Df(3R)J18* and *dKdm2^{d00170}* homozygous mutants (Fig. 4H). Taken together, these results suggest that despite both mRNA and protein of dKDM2 are very low or undetectable in the class II mutant alleles of *dKdm2* gene, they affect the expression of its neighboring genes, which may be responsible for the pupal lethality in these mutant animals. It is technically difficult to rigorously exclude the possibility that the indirect effect of loss of both *dKdm2* and *beag*, together with over-expression of *Ada*, contributed to the pupal lethality in *Df(3R)J16* and *Df(3R)J18* homozygous mutants.

Furthermore, we performed similar analyses with four class III *dKdm2* alleles, including *dKdm2^{d06730}*, *dKdm2^{EY01336}*, *dKdm2^{F11.1}*, and *dKdm2^{KG04325}*. Despite insertions of large transposons in the third intron of *dKdm2* locus (Fig. S3), we observed that the levels of *dKdm2* and its neighboring genes are not significantly affected (Fig. S3A ~ S3D). Consistent with this observation, the levels of dKDM2 protein are also not affected in these alleles (Fig. S3E ~ S3G). Therefore, these class III alleles should not be considered as the mutant alleles of *dKdm2*.

Expression of *Kdm2* and its neighboring genes in trans-heterozygous mutants

Next, we performed similar analyses by focusing on a few trans-heterozygotic combinations that are fully viable. We observed that the exon 2 of *dKdm2* was undetectable in *Df(3R)J15/Df(3R)J16* (Fig. 5A), *Df(3R)J15/Df(3R)J18* (Fig. 5B), *Df(3R)J15/dKdm2^{DG12810}* (Fig. 5C) mutants, which is similar to *Df(3R)J15* homozygous mutants, while the exon 3 and exon 4 levels are normalized in *Df(3R)J15/Df(3R)J16* (Fig. 5A) and *Df(3R)J15/Df(3R)J18* (Fig. 5B) mutants, but not affected in *Df(3R)J15/dKdm2^{DG12810}* (Fig. 5C) mutants. The expression pattern of *dKdm2* neighboring genes (Fig. 5A ~ Fig. 5C) is consistent with expectations based on what we observed in homozygous mutants (Fig. 4). Similarly, we examined the *dKdm2* expression in *Df(3R)J16/Df(3R)J18* (Fig. 5D), *Df(3R)J16/dKdm2^{DG12810}* (Fig. 5E), and *Df(3R)J18/dKdm2^{DG12810}* (Fig. 5F) transheterozygous mutants, and we observed that all exons of *dKdm2* were undetectable in these combinations. The major difference among these three combinations is the expression of *beag* (Fig. 5D *vs.* Fig. 5E/F), which is deleted in *Df(3R)J16/Df(3R)J18* mutants. Unlike *Df(3R)J16/Df(3R)J18* mutants, *Df(3R)J16/dKdm2^{DG12810}* and *Df(3R)J18/dKdm2^{DG12810}* animals are fully viable (Table 1), suggesting that the pupal lethality of *Df(3R)J16/Df(3R)J18* heterozygous, as well as *Df(3R)J16* and *Df(3R)J18* homozygous mutants are likely due to loss of *beag* but not loss of *dKdm2* or ectopic gain of *Ada*. Moreover, we analyzed the expression of these genes in *Df(3R)J18/dKdm2^{d00170}* (Fig. 5G) and *dKdm2^{d00170}/dKdm2^{DG12810}* (Fig. 5H) and observed that *dKdm2* mRNA remains undetectable or low in these transheterozygous mutants. Therefore, these results do not support the idea of transvection in interpreting the complementation among the class I and the class II *dKdm2* alleles.

In addition, we examined the levels of dKDM2 protein in several heteroallelic combinations, including $Df(3R)J15/Df(3R)J16$, $Df(3R)J16/Df(3R)J18$, $Df(3R)J16/dKdm2^{d01700}$, $Df(3R)J18/dKdm2^{DG12810}$, $dKdm2^{d00170}/dKdm2^{DG12810}$, $Df(3R)J15/ dKdm2^{DG12810}$, $dKdm2^{d00170}/dKdm2^{f02828}$, and $dKdm2^{EP3093}/dKdm2^{f02828}$ during the third instar wandering stage. Using the $Df(3R)J16$ homozygous as a control, we observed that dKDM2 proteins are undetectable in these transheterozygous mutants, except the $dKdm2^{EP3093}/dKdm2^{f02828}$ mutants (Fig. 5I). These results are consistent to $dKdm2$ RNA levels in these heteroallelic combinatins (Fig. S5). Taken together, the results from these genetic, molecular and biochemical analyses argue against the possibility of transvection between the class I and class II $dKdm2$ alleles, thus the most parsimonious explanation of these observations is that $dKdm2$ may not required for fly viability.

Potential second-site mutation(s) in the class I and class II *dKdm2* alleles

One observation against the conclusion that $dKdm2$ is not essential for normal development is that several of the homozygous mutants of class I and class II $dKdm2$ alleles are lethal during L1, L2 or pupal stages (Table 1). For example, the homozygous mutants of $dKdm2^{f02828}$ and $dKdm2^{EP3093}$ alleles are lethal during L1 (Table 1). Similarly, $dKdm2^{d00170}$ and $dKdm2^{DG12810}$ are lethal during L3 and pupal stages, and these two alleles disrupted $dKdm2$, but have little or only mild effects on $dKdm2$ neighboring genes (Fig. 4E and Fig. 4F). If $dKdm2$ is not required for normal development, one possible explanation for the lethality of these alleles is that they are caused by recessive mutation(s) in the genetic backgrounds of these alleles.

To remove the potential recessive mutations in these four alleles, we outcrossed them with wild-type (w^{1118} strain) flies for four generations and the cleaned alleles are denoted by adding '#' after these alleles (Table 2). We observed that instead of lethal during larval stage (L1 or L3), the $dKdm2^{EP3093\#}$ and $dKdm2^{d00170\#}$ homozygous mutants become fully viable (Table 2), suggesting that the original transposon insertion lines indeed harbor unknown second site mutation(s). The presence of the transposon insertions of these alleles in the cleaned homozygous mutants was verified again by PCR and qRT-PCR analyses (Fig. S6). In addition, unlike the L1 stage lethal of the original line, $dKdm2^{f02828\#}$ homozygous mutants are lethal during L3 and pupal stage, this improvement also suggest additional mutations in the genetic background. However, the $dKdm2^{DG12810\#}$ homozygous mutants are still pupal lethal. Perhaps the recessive lethal mutations are very close to $dKdm2^{f02828\#}$ and $dKdm2^{DG12810\#}$ alleles and four generations of outcrossing was not sufficient to completely separate the unknown recessive lesions from these two $dKdm2$ alleles. This possibility is supported by the observation that $dKdm2^{f02828\#}/Df(3R)J15$ animals are fully viable (Table 2), instead of L1 lethal prior to outcrossing (Table 1).

In addition, we outcrossed the $Df(3R)J15$ line and found that homozygotes of $Df(3R)J15\#$ allele become fully viable. The PCR verifications of two independently outcrossed $Df(3R)J15\#$ lines are shown Fig. 6A ~ Fig. 6D. Analysis of the mRNA levels of $dKdm2$ in the third instar homozygous $Df(3R)J15\#$ larvae (Fig. 6E) revealed similar expression pattern to the first instar larvae of the homozygous $Df(3R)J15$ mutants (Fig. 4B). $Df(3R)J15$ removes the exon 2 of $dKdm2$, which encodes the AA1~44 of dKDM2 protein (Fig. 3A).

The Western blot analysis did not reveal an extra truncated dKDM2 protein with 1301AA (exons 3~6) in *Df(3R)J15/Df(3R)J16* and *Df(3R)J15/ dKdm2^DG12810* larvae (Fig. 5I), indicating that *Df(3R)J15* is likely a *dKdm2* null allele.

Effects of loss of *dKdm2* on histone lysine modifications

The functions of KDM2 in *Drosophila* and mammalian cells are still controversial. The mammalian KDM2A and KDM2B were found to function as an H3K36me2/me1 demethylase (He et al., 2008; Lagarou et al., 2008; Tsukada et al., 2006; Tzatsos et al., 2009), but no effect of KDM2B on H3K4me3 was observed (He et al., 2008). However, KDM2B was also reported to demethylate H3K4me3 instead (Frescas et al., 2007; Janzer et al., 2012; Tzatsos et al., 2009). Similarly, data from *Drosophila* also appear contradictory: dKDM2 was reported to target H3K36me2, but not H3K36me1/me3 and H3K4me3, when dKDM2 is depleted in S2 cells (Lagarou et al., 2008); however, dKDM2 was also reported to target H3K4me3 in larvae with *dKdm2* -depleted by expressing dsRNA targeting *dKdm2* under control of *act5C-Gal4*, but has no effect on H3K4me2, H3K9me2 and H3K36me2 (Kavi and Birchler, 2009). Perhaps, the differences are dues to different experimental approaches. For example, the data from mammalian cells are based on overexpression of wild-type KDM2B, and the effects of depletion of KDM2B on histone methylation remain unclear. Alternatively, KDM2 may present in different protein complexes at different developmental stages or in different tissues.

To clarify the exact role of dKDM2 *in vivo*, it is important to analyze the status of histone methylation in loss of *dKdm2* mutant animals. Therefore, we first focused on two homozygous mutants of class II *dKdm2* alleles, *Df(3R)J16* and *Df(3R)J18*. As shown in Fig. 7A, we observed that the levels of H3K36me1/2/3 are increased in the *Df(3R)J16* and *Df(3R)J18* homozygous mutants during the third instar larval stage. In contrast, the levels of H3K4me3 were weakly affected in the mutants, while the levels of H3K4me1/me2, H3K9me2 and H3K27me2/me3 were not affected in the mutants compared to the control (Fig. 7A). Similar observations were made with *dKdm2^DG12810*, and to a less extent, *dKdm2^d00170* homozygous mutants (Fig. 7B). In addition, we analyzed the histone modification in *dKdm2^DG12810/Df(3R)J16* and *dKdm2^DG12810/Df(3R)J18* transheterozygous larvae and found that only H3K36me1/2 are affected (Fig. 7C).

For the following two reasons, we cannot rigorously conclude that the effects of *Df(3R)J16* and *Df(3R)J18* on H3K4me and H3K36me are due to loss of dKDM2: first, the *Df(3R)J16* and *Df(3R)J18* homozygotes are lethal during late L3 and pupal stage (Table 1), both of these alleles delete both *dKdm2* and *beag* but simultaneously upregulate the expression of *Ada* (Fig. 3A, Fig. 4C and Fig. 4D). Second, *beag* encodes a spliceosomal protein that regulates synapse development and neurotransmitter release, and the null mutants (*beag^1/ beag^1*) are semilethal with over 60% of the homozygous mutants die (Beck et al., 2012). The exact cause for lethality of the *Df(3R)J16* and *Df(3R)J18* homozygotes is a thorny problem, which can be caused by loss of *dKdm2* and *beag*, overexpression of *Ada*, potential recessive mutations in the background, or different combinations of these issues.

To complement these *in vivo* analyses, therefore, we examined the effect of depletion dKDM2 using two different dsRNAs specifically targeting dKDM2 in cultured *Drosophila*

S2- DRSC cells. These two dsRNAs are effective in depleting dKDM2 protein after 4 days of treatment (Fig. 7D). Compared to the control cells that were treated with shRNA targeting *white* gene, depletion of dKDM2 did not affect the methylation levels of H3K4me1/me2/ me3, H3K36me1/me2/me3, H3K9me2, or H3K27me2/me3 (Fig. 7E). Perhaps the residual dKDM2 proteins are sufficient to maintain the normal levels of methylation at these sites. Taken together, these observations show that the role of dKDM2 in regulating H3K4me and H3K36me appears rather weak during the larvae stage, suggesting that dKDM2 may be redundant with other histone lysine demthylases during development.

DISCUSSION

The past two decades have witnessed an explosion of information regarding how histone lysine methyltransferases and demethylases, especially the biochemical mechanisms underlying the activities of these enzymes, contribute to the regulation of gene expression. However, the regulation and functions of these enzymes during development and different physiological and pathological contexts remain poorly understood. Here we report our developmental genetic analyses of multiple mutant alleles of the lysine demethylase KDM2 in *Drosophila, dKdm2*. We found that dKDM2 is a nuclear protein, and both the mRNA and protein levels of dKDM2 fluctuate during *Drosophila* development. In addition, our molecular and genetic analyses with multiple *dKdm2* alleles suggest that dKDM2 is not required for viability. Furthermore, the effects of loss of dKDM2 on H3K4me3 and H3K36me are rather marginal at the third instar larval stage. We did not observe any changes of methylation status on H3K4me1/me2, H3K9me2 and H3K27me2/me3 in *dKdm2* mutant larvae.

That *dKdm2* is actually not required for viability of *Drosophila* is supported by the complementation genetic tests among all *dKdm2* alleles (Table 1 and Table 2), as well as the molecular and biochemical analyses of the levels of *dKdm2* mRNA and protein levels in both homozygous and transheterzygous combinations of the *dKdm2* alleles (Fig. 4, Fig. 5, Fig. S5 and Fig. S6). However, one would expect that *dKdm2* is an essential gene for normal *Drosophila* development for the following reasons: First, dKDM2 regulates methylation status of H3K36me2 (Lagarou et al., 2008), which plays important roles in regulating transcription elongation and DNA mismatch repair (Buratowski and Kim, 2010; Li et al., 2013). Second, dKDM2 was identified as a subunit of the dRAF (dRING-associated factors dRING-associated factors) complex, and is thought to play pivotal roles to mediate H3K36me2 demethylation and is required for H2A ubiquitination by dRING in the dRAF complex (Lagarou et al., 2008). Third, as summarized in the Introduction, the mammalian KDM2 homologs have been shown to regulate stem cell differentiation and dysregulation of them are linked to a number of human cancers. Therefore, the conclusion that *dKdm2* is not required for viability raises two major questions that warrant further discussion.

First, if *dKdm2* is not essential for viability of *Drosophila*, technically how can we explain the lethality of the class I and the class II *dKdm2* mutants? The class I alleles include three *dKdm2* alleles (Table 1). After outcrossing with the *w^1118^* line, *dKdm2^EP3093#^* and *Df(3R)J15#* mutants become fully viable, suggesting that the lethality of *dKdm2^EP3093^* and *Df(3R)J15* homozygotes (the original insertion or deletion line, respectively) during L1 is

caused by the second site lethal mutation(s). Consistent to this notion, the homozygous mutants of cleaned *dKdm2^{f02828#}* allele are lethal during L3 and pupal stage, instead of the L1 lethal in the original *dKdm2^{f02828}* allele (Table 1 and Table 2), suggesting that the additional mutation(s) could be too close to *dKdm2^{f02828}* to be removed by four generations of outcrossing. Both the original *Df(3R)J15* homozygotes, which are also lethal during L1 stage (Table 1), and the outcrossed *Df(3R)J15#* homozygotes have significantly elevated expression of the exon 3 to exon 6 but not exon 2 of the *dKdm2* gene (Fig. S3B), raising the possibility that the ectopic expression of a truncated dKDM2 fragment may be detrimental to normal development. However, our immunoblots data of *Df(3R)J15/Df(3R)J16* and *Df(3R)J15/dKdm2^{DG12810}* transheterozygous mutants (Fig. 5I) argue against this possibility. Because *dKdm2^{f02828#}/Df(3R)J15* and *Df(3R)J15#* homozygous animals are fully viable (Table 2), we favor the alternative explanation that the L1 lethality of the *dKdm2^{f02828}* and *Df(3R)J15* mutants is likely due to similar second-site mutations in their shared genetic background (Fig. 3).

The class II allele (*Df(3R)J16*, *Df(3R)J18*, *dKdm2^{d00170}*, and *dKdm2^{DG12810}*) mutants are lethal during L3 and pupal stages (Table 1). Rather than disruption of *dKdm2* alone, the lethality of the *Df(3R)J16/Df(3R)J18* animals is likely caused by the deletion of *beag* gene and overexpression of Ada (Fig. 4), since *Df(3R)J16* and *Df(3R)J18* delete not only *dKdm2* but also its neighboring gene *beag* (Fig. 2A, Fig. 4C and Fig. 4D). Similar to *dKdm2^{EP3093#}* mutants, the cleaned *dKdm2^{d00170#}* mutants are also fully viable, supporting that the original *dKdm2^{d00170}* allele harbors recessive lethal mutation(s) in their genetic background. We note that four generations of outcrossing with *dKdm2^{DG12810}* allele did not improve viability, and we speculate that such lethal mutations may be close to *dKdm2* and four generations of outcrossing was not sufficient to eliminate them. Although these analyses suggest that *dKdm2* gene is not be required for viability, we note that none of existing *dKdm2* mutant alleles is perfect to rigorous test this, which ultimately requires generation of null *dKdm2* alleles without affecting its neighboring genes in the future.

The second major question is: if dKDM2 is not required for the viability of *Drosophila*, why is *dKdm2* not lost during evolution and what are the selection pressures that keep DKM2 proteins so conserved in multicellular organisms? We think that there are two possible explanations. First, it is possible that dKDM2 is redundant to other histone demethylases, such as dKDM4A (CG15835) and dKDM4B (CG33182). Besides KDM2, KDM4 and KDM8 (JMJD5) have been reported to demethylate H3K36me2 in mammals (Crona et al., 2013; Hsia et al., 2010; Ishimura et al., 2012; Lin et al., 2012). Although KDM8 homolog does not exist in *Drosophila*, dKDM4A has been reported to demethylate H3K36me2/me3 *in vitro* (Lin et al., 2008), and its paralog dKDM4B targets both H3K36me2/me3 and H3K9me2/me3 (Lin et al., 2008; Tsurumi et al., 2013). Interestingly, the *dKdm4A* null (*dKdm4A*) homozygous mutants are fully viable, fertile and do not display any obvious developmental defects (Crona et al., 2013). Similarly, homozygous mutants of another amorphic allele *dKdm4A^{KG04636}*, a P-element insertion within the first exon of *dKdm4A*, are also fully viable, but have reduced lifespan in males (Lorbeck et al., 2010). It is thus possible that dKDM2 is redundant with histone lysine demethylases such as dKDM4A or dKDM4B, in regulating the methylation status on H3K36, which would explain why we

only observed rather mild effect of dKDM2 mutation on H3K36me and H3K4me during the larval stage. It was previously reported that depleting dKDM2 with dsRNA in S2 cells for 4 days led to increased H3K36me2 levels (Lagarou et al., 2008). For reasons that we do not understand, our depletion of dKDM2 using two different dsRNAs (648bp and 956bp, respectively) failed to show any effect on histone modifications (Fig. 7B). Perhaps, the dsRNA depletion of dKDM2 in S2 cells did not reach the threshold for us to detect the effect on histone modification, or due to different expression of histone lysine demethylases between the two *Drosophila* cell lines. Nevertheless, the potential redundancy between dKDM2 and other lysine demethylases may increase the robustness of gene regulatory networks during development.

Second, it is also possible that dKDM2 is required to respond to stresses, such as oxidative and genotoxic stresses, considering that phosphoproteomic analysis has identified seven serine residues and one tyrosine residue of dKDM2 are phosphorylated in *Drosophila* embryos (Zhai et al., 2008). However, it is completely unknown as to which kinases phosphorylate dKDM2 at what biological contexts. Interestingly, *dKdm2* mutants are defective in ethanol metabolism and sensitive to ethanol-induced hyperactivity (Devineni et al., 2011). In addition, H3K36me3 was shown recently to play a critical role during initiation of DNA mismatch repair (Li et al., 2013). Considering the role of KDM2 in regulating H3K36 methylation, it will be interesting to examine whether KDM2 is involved in the maintenance of genome stability in response to genotoxic and other stresses. Based on our genetic and biochemical analyses of the *dKdm2* alleles, it will be important to examine if dKDM2 is redundant with other histone demethylases and whether dKDM2 is involved in stress responses in the future.

Supplementary Material

Refer to Web version on PubMed Central for supplementary material.

Acknowledgments

LITERATURE CITED

Allis CD, Berger SL, Cote J, Dent S, Jenuwien T, Kouzarides T, Pillus L, Reinberg D, Shi Y, Shiekhattar R, Shilatifard A, Workman J, Zhang Y. New nomenclature for chromatin-modifying enzymes. Cell. 2007; 131:633–636. [PubMed: 18022353]

Altschul SF, Madden TL, Schaffer AA, Zhang J, Zhang Z, Miller W, Lipman DJ. Gapped BLAST and PSI-BLAST: a new generation of protein database search programs. Nucleic Acids Res. 1997; 25:3389–3402. [PubMed: 9254694]

Bannister AJ, Kouzarides T. Regulation of chromatin by histone modifications. Cell Res. 2011; 21:381–395. [PubMed: 21321607]

Beck ES, Gasque G, Imlach WL, Jiao W, Jiwon Choi B, Wu PS, Kraushar ML, McCabe BD. Regulation of Fasciclin II and synaptic terminal development by the splicing factor beag. J Neurosci. 2012; 32:7058–7073. [PubMed: 22593074]

Bellen HJ, Levis RW, Liao G, He Y, Carlson JW, Tsang G, Evans-Holm M, Hiesinger PR, Schulze KL, Rubin GM, Hoskins RA, Spradling AC. The BDGP gene disruption project: single transposon insertions associated with 40% of Drosophila genes. Genetics. 2004; 167:761–781. [PubMed: 15238527]

Blackledge NP, Zhou JC, Tolstorukov MY, Farcas AM, Park PJ, Klose RJ. CpG islands recruit a histone H3 lysine 36 demethylase. Mol Cell. 2010; 38:179–190. [PubMed: 20417597]

Buratowski S, Kim T. The role of cotranscriptional histone methylations. Cold Spring Harb Symp Quant Biol. 2010; 75:95–102. [PubMed: 21447819]

Chi P, Allis CD, Wang GG. Covalent histone modifications--miswritten, misinterpreted and mis-erased in human cancers. Nat Rev Cancer. 2010; 10:457–469. [PubMed: 20574448]

Cloos PA, Christensen J, Agger K, Helin K. Erasing the methyl mark: histone demethylases at the center of cellular differentiation and disease. Genes Dev. 2008; 22:1115–1140. [PubMed: 18451103]

Crona F, Dahlberg O, Lundberg LE, Larsson J, Mannervik M. Gene regulation by the lysine demethylase KDM4A in Drosophila. Dev Biol. 2013; 373:453–463. [PubMed: 23195220]

Devineni AV, McClure KD, Guarnieri DJ, Corl AB, Wolf FW, Eddison M, Heberlein U. The genetic relationships between ethanol preference, acute ethanol sensitivity, and ethanol tolerance in Drosophila melanogaster. Fly (Austin). 2011; 5:191–199. [PubMed: 21750412]

Dimova DK, Stevaux O, Frolov MV, Dyson NJ. Cell cycle-dependent and cell cycle-independent control of transcription by the Drosophila E2F/RB pathway. Genes Dev. 2003; 17:2308–2320. [PubMed: 12975318]

Dui W, Lu W, Ma J, Jiao R. A systematic phenotypic screen of F-box genes through a tissue-specific RNAi-based approach in Drosophila. J Genet Genomics. 2012; 39:397–413. [PubMed: 22884096]

Frescas D, Guardavaccaro D, Bassermann F, Koyama-Nasu R, Pagano M. JHDM1B/FBXL10 is a nucleolar protein that represses transcription of ribosomal RNA genes. Nature. 2007; 450:309–313. [PubMed: 17994099]

Gohl DM, Silies MA, Gao XJ, Bhalerao S, Luongo FJ, Lin CC, Potter CJ, Clandinin TR. A versatile in vivo system for directed dissection of gene expression patterns. Nat Methods. 2011; 8:231–237. [PubMed: 21473015]

Graveley BR, Brooks AN, Carlson JW, Duff MO, Landolin JM, Yang L, Artieri CG, van Baren MJ, Boley N, Booth BW, Brown JB, Cherbas L, Davis CA, Dobin A, Li R, Lin W, Malone JH, Mattiuzzo NR, Miller D, Sturgill D, Tuch BB, Zaleski C, Zhang D, Blanchette M, Dudoit S, Eads B, Green RE, Hammonds A, Jiang L, Kapranov P, Langton L, Perrimon N, Sandler JE, Wan KH, Willingham A, Zhang Y, Zou Y, Andrews J, Bickel PJ, Brenner SE, Brent MR, Cherbas P, Gingeras TR, Hoskins RA, Kaufman TC, Oliver B, Celniker SE. The developmental transcriptome of Drosophila melanogaster. Nature. 2011; 471:473–479. [PubMed: 21179090]

Greer EL, Shi Y. Histone methylation: a dynamic mark in health, disease and inheritance. Nat Rev Genet. 2012; 13:343–357. [PubMed: 22473383]

He J, Kallin EM, Tsukada Y, Zhang Y. The H3K36 demethylase Jhdm1b/Kdm2b regulates cell proliferation and senescence through p15(Ink4b). Nat Struct Mol Biol. 2008; 15:1169–1175. [PubMed: 18836456]

He J, Nguyen AT, Zhang Y. KDM2b/JHDM1b, an H3K36me2-specific demethylase, is required for initiation and maintenance of acute myeloid leukemia. Blood. 2011; 117:3869–3880. [PubMed: 21310926]

Hsia DA, Tepper CG, Pochampalli MR, Hsia EY, Izumiya C, Huerta SB, Wright ME, Chen HW, Kung HJ, Izumiya Y. KDM8, a H3K36me2 histone demethylase that acts in the cyclin A1 coding region to regulate cancer cell proliferation. Proc Natl Acad Sci U S A. 2010; 107:9671–9676. [PubMed: 20457893]

Huet F, Lu JT, Myrick KV, Baugh LR, Crosby MA, Gelbart WM. A deletion-generator compound element allows deletion saturation analysis for genomewide phenotypic annotation. Proc Natl Acad Sci U S A. 2002; 99:9948–9953. [PubMed: 12096187]

Ishimura A, Minehata K, Terashima M, Kondoh G, Hara T, Suzuki T. Jmjd5, an H3K36me2 histone demethylase, modulates embryonic cell proliferation through the regulation of Cdkn1a expression. Development. 2012; 139:749–759. [PubMed: 22241836]

Janzer A, Stamm K, Becker A, Zimmer A, Buettner R, Kirfel J. The H3K4me3 histone demethylase Fbxl10 is a regulator of chemokine expression, cellular morphology, and the metabolome of fibroblasts. J Biol Chem. 2012; 287:30984–30992. [PubMed: 22825849]

Ji JY, Miles WO, Korenjak M, Zheng Y, Dyson NJ. In vivo regulation of E2F1 by Polycomb group genes in Drosophila. G3 (Bethesda). 2012; 2:1651–1660. [PubMed: 23275887]

Jin J, Cardozo T, Lovering RC, Elledge SJ, Pagano M, Harper JW. Systematic analysis and nomenclature of mammalian F-box proteins. Genes Dev. 2004; 18:2573–2580. [PubMed: 15520277]

Jones MA, Covington MF, DiTacchio L, Vollmers C, Panda S, Harmer SL. Jumonji domain protein JMJD5 functions in both the plant and human circadian systems. Proc Natl Acad Sci U SA. 2010; 107:21623–21628.

Joshi AA, Struhl K. Eaf3 chromodomain interaction with methylated H3-K36 links histone deacetylation to Pol II elongation. Mol Cell. 2005; 20:971–978. [PubMed: 16364921]

Kavi HH, Birchler JA. Drosophila KDM2 is a H3K4me3 demethylase regulating nucleolar organization. BMC Res Notes. 2009; 2:217. [PubMed: 19852816]

Kennison JA, Southworth JW. Transvection in Drosophila. Adv Genet. 2002; 46:399–420. [PubMed: 11931232]

Koyama-Nasu R, David G, Tanese N. The F-box protein Fbl10 is a novel transcriptional repressor of c-Jun. Nat Cell Biol. 2007; 9:1074–1080. [PubMed: 17704768]

Lagarou A, Mohd-Sarip A, Moshkin YM, Chalkley GE, Bezstarosti K, Demmers JA, Verrijzer CP. dKDM2 couples histone H2A ubiquitylation to histone H3 demethylation during Polycomb group silencing. Genes Dev. 2008; 22:2799–2810. [PubMed: 18923078]

Li B, Carey M, Workman JL. The role of chromatin during transcription. Cell. 2007; 128:707–719. [PubMed: 17320508]

Li F, Mao G, Tong D, Huang J, Gu L, Yang W, Li GM. The histone mark H3K36me3 regulates human DNA mismatch repair through its interaction with MutSalpha. Cell. 2013; 153:590–600. [PubMed: 23622243]

Lin CH, Li B, Swanson S, Zhang Y, Florens L, Washburn MP, Abmayr SM, Workman JL. Heterochromatin protein 1a stimulates histone H3 lysine 36 demethylation by the Drosophila KDM4A demethylase. Mol Cell. 2008; 32:696–706. [PubMed: 19061644]

Lin CH, Paulson A, Abmayr SM, Workman JL. HP1a targets the Drosophila KDM4A demethylase to a subset of heterochromatic genes to regulate H3K36me3 levels. PLoS One. 2012; 7:e39758. [PubMed: 22761891]

Lohse B, Kristensen JL, Kristensen LH, Agger K, Helin K, Gajhede M, Clausen RP. Inhibitors of histone demethylases. Bioorg Med Chem. 2011; 19:3625–3636. [PubMed: 21596573]

Lorbeck MT, Singh N, Zervos A, Dhatta M, Lapchenko M, Yang C, Elefant F. The histone demethylase Dmel\Kdm4A controls genes required for life span and male-specific sex determination in Drosophila. Gene. 2010; 450:8–17. [PubMed: 19786080]

Lu T, Jackson MW, Wang B, Yang M, Chance MR, Miyagi M, Gudkov AV, Stark GR. Regulation of NF-kappaB by NSD1/FBXL11-dependent reversible lysine methylation of p65. Proc Natl Acad Sci U S A. 2010; 107:46–51. [PubMed: 20080798]

Myrick KV, Huet F, Mohr SE, Alvarez-Garcia I, Lu JT, Martin TM, Crosby MA, Gelbart WM. Deletion Generator Project genomic insertion collection. 2005

Nottke A, Colaiacovo MP, Shi Y. Developmental roles of the histone lysine demethylases. Development. 2009; 136:879–889. [PubMed: 19234061]

Parks AL, Cook KR, Belvin M, Dompe NA, Fawcett R, Huppert K, Tan LR, Winter CG, Bogart KP, Deal JE, Deal-Herr ME, Grant D, Marcinko M, Miyazaki WY, Robertson S, Shaw KJ, Tabios M, Vysotskaia V, Zhao L, Andrade RS, Edgar KA, Howie E, Killpack K, Milash B, Norton A, Thao D, Whittaker K, Winner MA, Friedman L, Margolis J, Singer MA, Kopczynski C, Curtis D, Kaufman TC, Plowman GD, Duyk G, Francis-Lang HL. Systematic generation of high-resolution

deletion coverage of the Drosophila melanogaster genome. Nat Genet. 2004; 36:288–292. [PubMed: 14981519]

Pfau R, Tzatsos A, Kampranis SC, Serebrennikova OB, Bear SE, Tsichlis PN. Members of a family of JmjC domain-containing oncoproteins immortalize embryonic fibroblasts via a JmjC domain-dependent process. Proc Natl Acad Sci U S A. 2008; 105:1907–1912. [PubMed: 18250326]

Rotili D, Mai A. Targeting Histone Demethylases: A New Avenue for the Fight against Cancer. Genes Cancer. 2011; 2:663–679. [PubMed: 21941621]

Sanchez C, Sanchez I, Demmers JA, Rodriguez P, Strouboulis J, Vidal M. Proteomics analysis of Ring1B/Rnf2 interactors identifies a novel complex with the Fbxl10/Jhdm1B histone demethylase and the Bcl6 interacting corepressor. Mol Cell Proteomics. 2007; 6:820–834. [PubMed: 17296600]

Sarris M, Nikolaou K, Talianidis I. Context-specific regulation of cancer epigenomes by histone and transcription factor methylation. Oncogene. 2013

Smolle M, Workman JL. Transcription-associated histone modifications and cryptic transcription. Biochim Biophys Acta. 2013; 1829:84–97. [PubMed: 22982198]

Suzuki T, Minehata K, Akagi K, Jenkins NA, Copeland NG. Tumor suppressor gene identification using retroviral insertional mutagenesis in Blm-deficient mice. EMBO J. 2006; 25:3422–3431. [PubMed: 16858412]

Tamura K, Peterson D, Peterson N, Stecher G, Nei M, Kumar S. MEGA5: molecular evolutionary genetics analysis using maximum likelihood, evolutionary distance, and maximum parsimony methods. Mol Biol Evol. 2011; 28:2731–2739. [PubMed: 21546353]

Tanaka Y, Okamoto K, Teye K, Umata T, Yamagiwa N, Suto Y, Zhang Y, Tsuneoka M. JmjC enzyme KDM2A is a regulator of rRNA transcription in response to starvation. EMBO J. 2010; 29:1510–1522. [PubMed: 20379134]

Tang, W-JY. Blot-affinity purification of antibodies. In: Asai, DJ., editor. Methods in Cell Biology: Antibodies in Cell Biology. Academic Press; 1993. p. 95-104.

Thibault ST, Singer MA, Miyazaki WY, Milash B, Dompe NA, Singh CM, Buchholz R, Demsky M, Fawcett R, Francis-Lang HL, Ryner L, Cheung LM, Chong A, Erickson C, Fisher WW, Greer K, Hartouni SR, Howie E, Jakkula L, Joo D, Killpack K, Laufer A, Mazzotta J, Smith RD, Stevens LM, Stuber C, Tan LR, Ventura R, Woo A, Zakrajsek I, Zhao L, Chen F, Swimmer C, Kopczynski C, Duyk G, Winberg ML, Margolis J. A complementary transposon tool kit for Drosophila melanogaster using P and piggyBac. Nat Genet. 2004; 36:283–287. [PubMed: 14981521]

Timp W, Feinberg AP. Cancer as a dysregulated epigenome allowing cellular growth advantage at the expense of the host. Nat Rev Cancer. 2013; 13:497–510. [PubMed: 23760024]

Tsukada Y, Fang J, Erdjument-Bromage H, Warren ME, Borchers CH, Tempst P, Zhang Y. Histone demethylation by a family of JmjC domain-containing proteins. Nature. 2006; 439:811–816. [PubMed: 16362057]

Tsurumi A, Dutta P, Yan SJ, Sheng R, Li WX. Drosophila Kdm4 demethylases in histone H3 lysine 9 demethylation and ecdysteroid signaling. Sci Rep. 2013; 3:2894. [PubMed: 24100631]

Tzatsos A, Paskaleva P, Ferrari F, Deshpande V, Stoykova S, Contino G, Wong KK, Lan F, Trojer P, Park PJ, Bardeesy N. KDM2B promotes pancreatic cancer via Polycomb-dependent and -independent transcriptional programs. J Clin Invest. 2013; 123:727–739. [PubMed: 23321669]

Tzatsos A, Pfau R, Kampranis SC, Tsichlis PN. Ndy1/KDM2B immortalizes mouse embryonic fibroblasts by repressing the Ink4a/Arf locus. Proc Natl Acad Sci U S A. 2009; 106:2641–2646. [PubMed: 19202064]

Wagner EJ, Carpenter PB. Understanding the language of Lys36 methylation at histone H3. Nat Rev Mol Cell Biol. 2012; 13:115–126. [PubMed: 22266761]

Wu CT, Morris JR. Transvection and other homology effects. Curr Opin Genet Dev. 1999; 9:237–246. [PubMed: 10322135]

Wu X, Johansen JV, Helin K. Fbxl10/Kdm2b recruits polycomb repressive complex 1 to CpG islands and regulates H2A ubiquitylation. Mol Cell. 2013; 49:1134–1146. [PubMed: 23395003]

Zentner GE, Henikoff S. Regulation of nucleosome dynamics by histone modifications. Nat Struct Mol Biol. 2013; 20:259–266. [PubMed: 23463310]

Zhai B, Villen J, Beausoleil SA, Mintseris J, Gygi SP. Phosphoproteome analysis of Drosophila melanogaster embryos. J Proteome Res. 2008; 7:1675–1682. [PubMed: 18327897]

Zhao X, Feng D, Wang Q, Abdulla A, Xie XJ, Zhou J, Sun Y, Yang ES, Liu LP, Vaitheesvaran B, Bridges L, Kurland IJ, Strich R, Ni JQ, Wang C, Ericsson J, Pessin JE, Ji JY, Yang F. Regulation of lipogenesis by cyclin-dependent kinase 8-mediated control of SREBP-1. J Clin Invest. 2012; 122:2417–2427. [PubMed: 22684109]

Zhou X, Ma H. Evolutionary history of histone demethylase families: distinct evolutionary patterns suggest functional divergence. BMC Evol Biol. 2008; 8:294. [PubMed: 18950507]

Highlights

- dKDM2 is a nuclear protein and its level fluctuates during *Drosophila* development.

- We generated three deletion lines that disrupt the *dKdm2* locus;

- Our complementation genetic tests suggest that dKDM2 is not required for viability.

- Loss of dKDM2 has weak effects on the methylation status of histone H3K36 or H3K4.
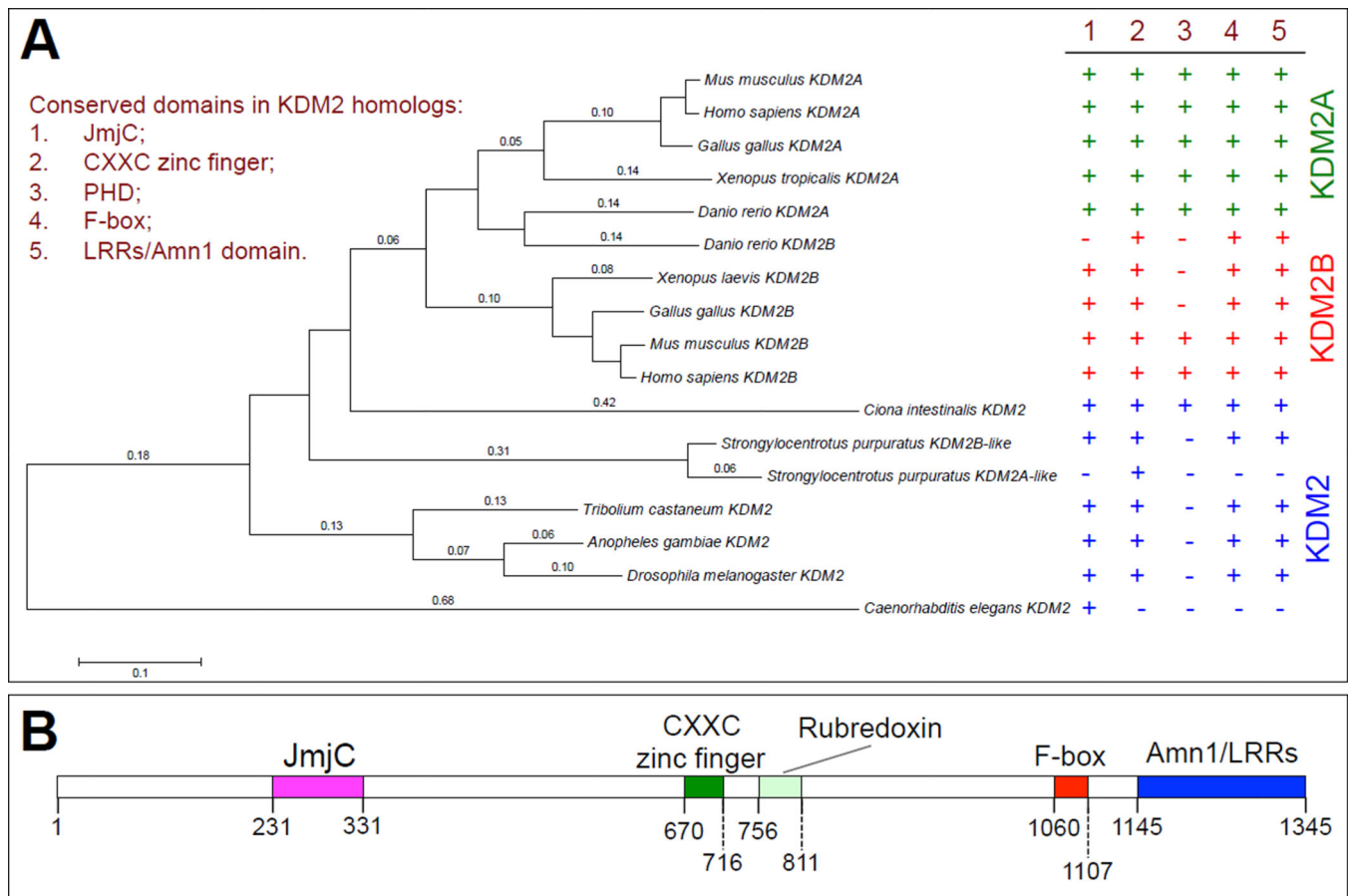
Figure 1. Characterization of the conserved protein domains in KDM2 homologs

(**A**) Phylogenetic tree of KDM2 proteins in multicellular animals. This tree was built with MEGA 5 by pairwise algorithm and the Neighbor-Joining algorithm. The right side summarizes the presence (marked with a '+') or absence (marked with a '−') of the conserved domains, including JmjC, CXXC zinc finger, PHD, F-box and LRRs/Amn1 domains. The NCBI Reference Sequence number and the protein-protein BLAST (BLASTp) search results for the putative conserved domains for each KDM2 homolog are presented in the Fig. S1. (**B**) The domain organization of dKDM2, note that except a clear PHD domain, all the other four major domains are present in dKDM2.
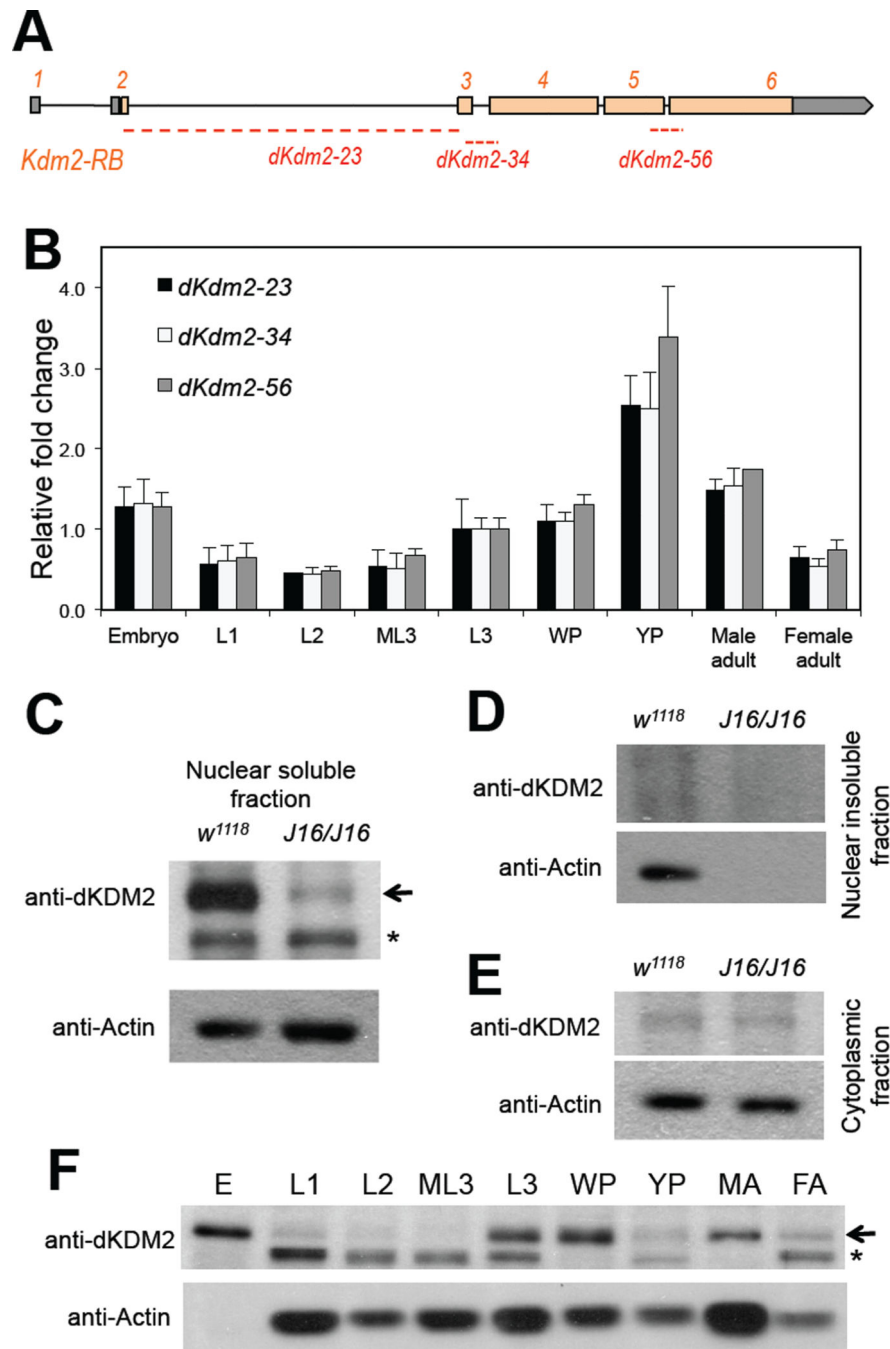
Figure 2. Expression of dKDM2 during noraml *Drosophila* development
(**A**) Schematic view of the *dKdm2* locus, showing the 6 exons with the coding exons in orange and UTR regions in grey. The three pairs of the primers used in qRT-PCR assay are shown below, and they all span the neighboring exons. (**B**) Quantitative RT-PCR analysis of relative expression of *dKdm2* mRNA during development. L1, first instar larvae; L2, second instar larvae; ML3, mid-third instar larvae; L3, third instar larvae; WP, white pupae; YP, yellow pupae. (**C ~ E**) Sub-cellular localization of the dKDM2 protein assayed with immunoblotting using a polyclonal antibody. dKDM2 protein is present in the nuclear

soluble fraction (**C**), and the *dKdm2* deletion line *Df(3R)J16* (see below) homozygous larvae was used as a negative control. dKDM2 protein is not present in the nuclear insoluble fraction (**D**) and the cytoplasmic fraction (**E**). (**F**) Levels of the dKDM2 protein in the nuclear soluble fraction of extract from different developmental stages. E, embryos; MA, male adults; FA, female adults. Equal total amount of proteins were loaded in each lane. The non-specific bands are marked with '*', and anti-Actin was used as a control.
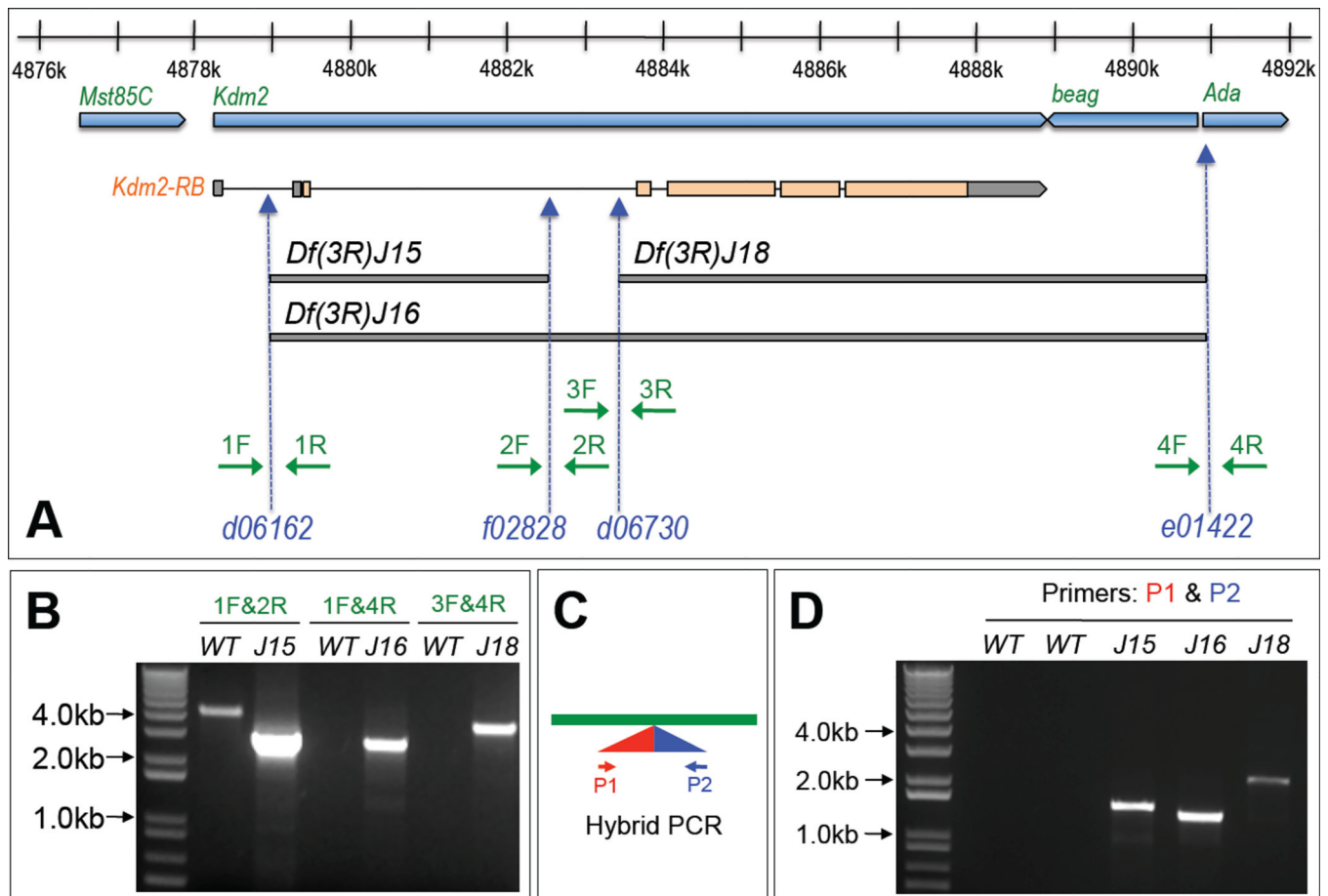
Figure 3. Generation and validation of three deletion lines *Df(2R)J15*, *Df(2R)J16*, and *Df(2R)J18* in the *dKdm2* locus

(**A**) Schematic representation of *dKdm2* locus and its neighboring genes including *Mst85C*, *beag* and *Ada*. The lower part of the figure shows the three new deletions (bars in grey) generated using four piggyBac insertion lines (blue) and the primers (green arrow) used for their validation. These deletions were validated by the two-sided PCR (**B**). Note that the extension time for PCR reaction was set so that only short templates (less than 5.0kb, when deletions occur in the deficiency lines) can be amplified. These deficiency lines were further verified using the hybrid PCR (**C**) and the results are shown in (**D**). In this assay, PCR products can be detected only when residual piggyBac transposons are present in the expected orientation.
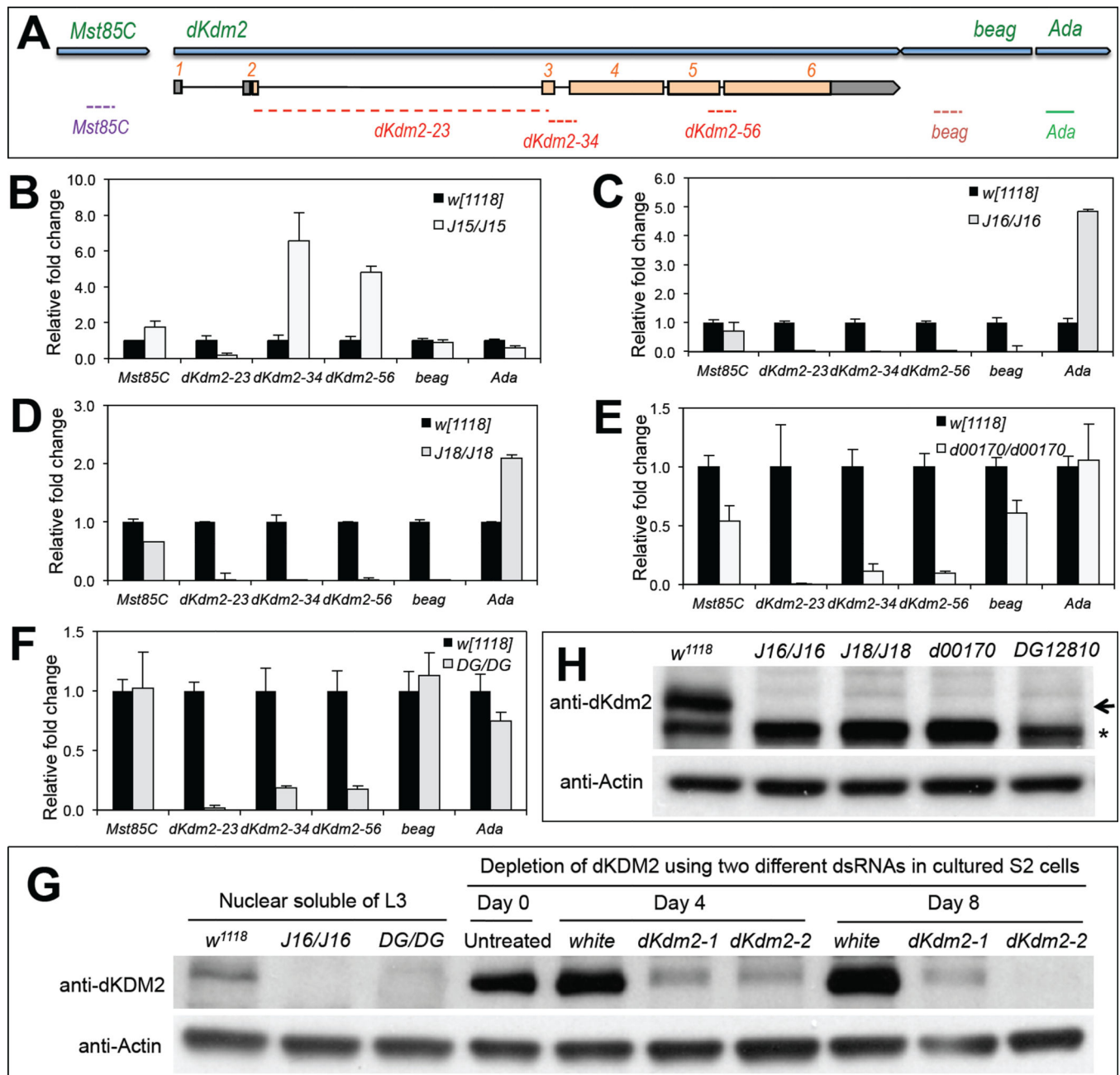
Figure 4. Effects of insertions and deletions of the class I and class II *dKdm2* alleles on the expression of *dKdm2* and its neighboring genes

(**A**) The location of the primers used for the qRT-PCR assay. Animals of the third instar at the wandering stage were used for the qRT-PCR (**C ~ F**) and immunoblots (**G** and **H**). The genotypes of the mutants include: w^{1118}; +; Df(3R)J15 (**B**, first instar laevar), w^{1118}; +; Df(3R)J16 (**C**), w^{1118}; +; Df(3R)J18 (**D**), w^{1118}; +; dKdm2^{d00170} (**E**), and w^{1118}; +; dKdm2^{DG12810} (**F**). (**G**) Western blot was used to demonstrate the specificity of the dKDM2 antiserum, note that the ~150kDa band is present in the control (w^{1118}) but not in the Df(3R)J16 and dKdm2^{DG12810} mutants. In addition, this band is present in untreated S2-DRSC cells or cells treated with dsRNA to *white* (control), but disappears in S2-DRSC cells

treated two different shRNAs targeting *dKdm2*. (**H**) Western blot of nuclear soluble proteins from the third instar larvae, showing that dDKM2 protein is undetectable in *Df(3R)J16*, *Df(3R)J18*, *dKdm2^{d00170}* or *dKdm2^{DG12810}* homozygous mutants.
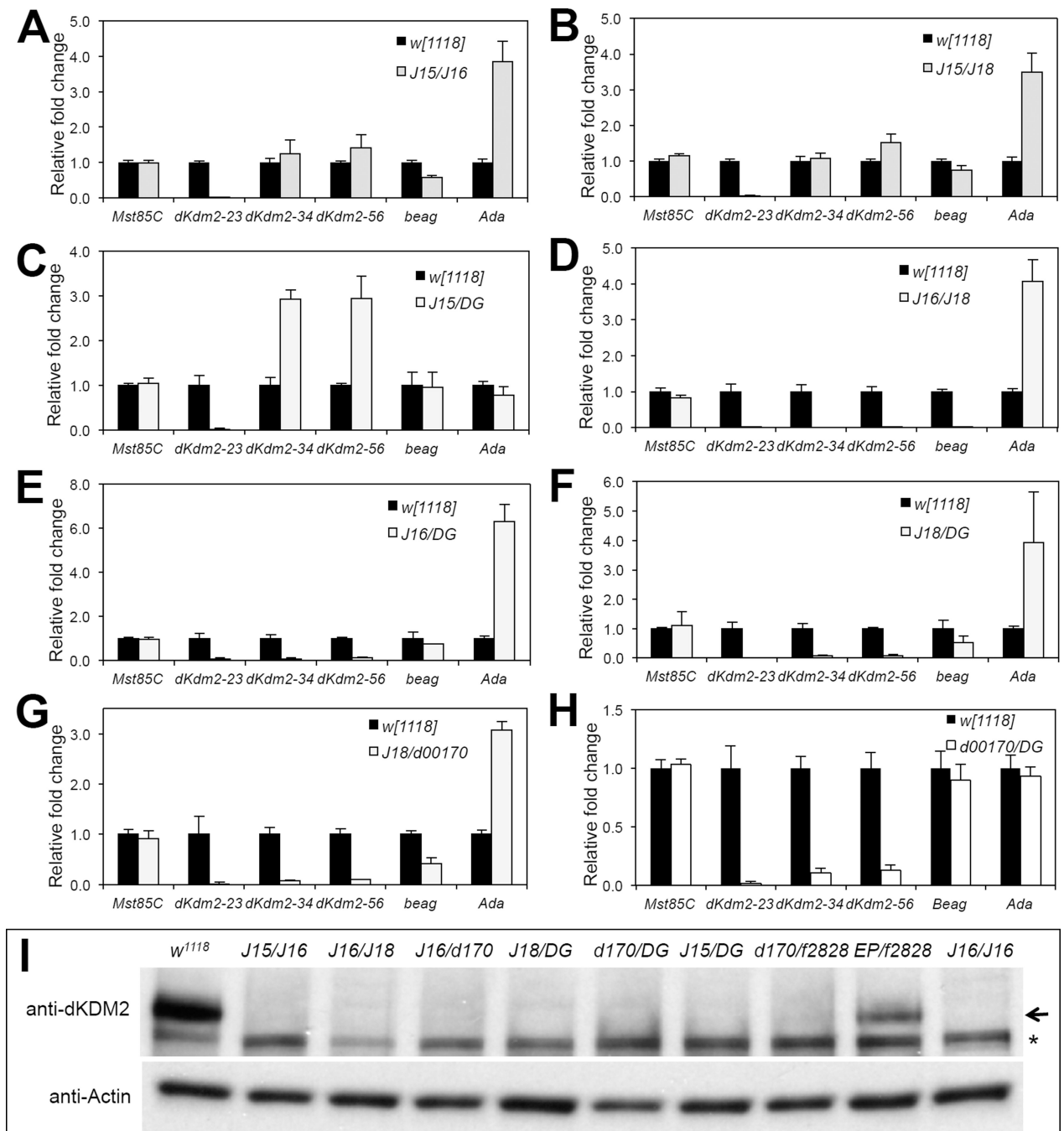
Figure 5. Expression of *dKdm2* and its neighboring genes in transheterozygous combination of several class I and class II *dKdm2* alleles

All animals were collected during the third instar at the wandering stage. The genotypes include: w^{1118}; +; Df(3R)J15/Df(3R)J16 (**A**), w^{1118}; +; Df(3R)J15/Df(3R)J18 (**B**), w^{1118}; +; Df(3R)J15/dKdm2^{DG12810} (**C**), Df(3R)J16/Df(3R)J18 (**D**), w^{1118}; +; Df(3R)J16/ dKdm2^{DG12810} (**E**), w^{1118}; +; Df(3R)J18/dKdm2^{DG12810} (**F**), w^{1118}; +; Df(3R)J18/ dKdm2^{d00170} (**G**), and w^{1118}; +; dKdm2^{d00170}/dKdm2^{DG12810} (**H**). (**I**) Western blot of nuclear soluble proteins from these transheterozygous mutant animals at the wandering

stage, note that dKDM2 protein was not detectable, except in the w^{1118}; +; $dKdm2^{EP3093}$/ $dKdm2^{f02828}$ mutants, which is due to the fact that the level of $dKdm2$ mRNA is not obviously affected in these mutants (Fig. S5E). The $Df(3R)J16$ homozygous mutants (denoted as "$J16/J16$") was used as a control; the arrow shows the dKDM2 band, and the non-specific band is marked with a "*".
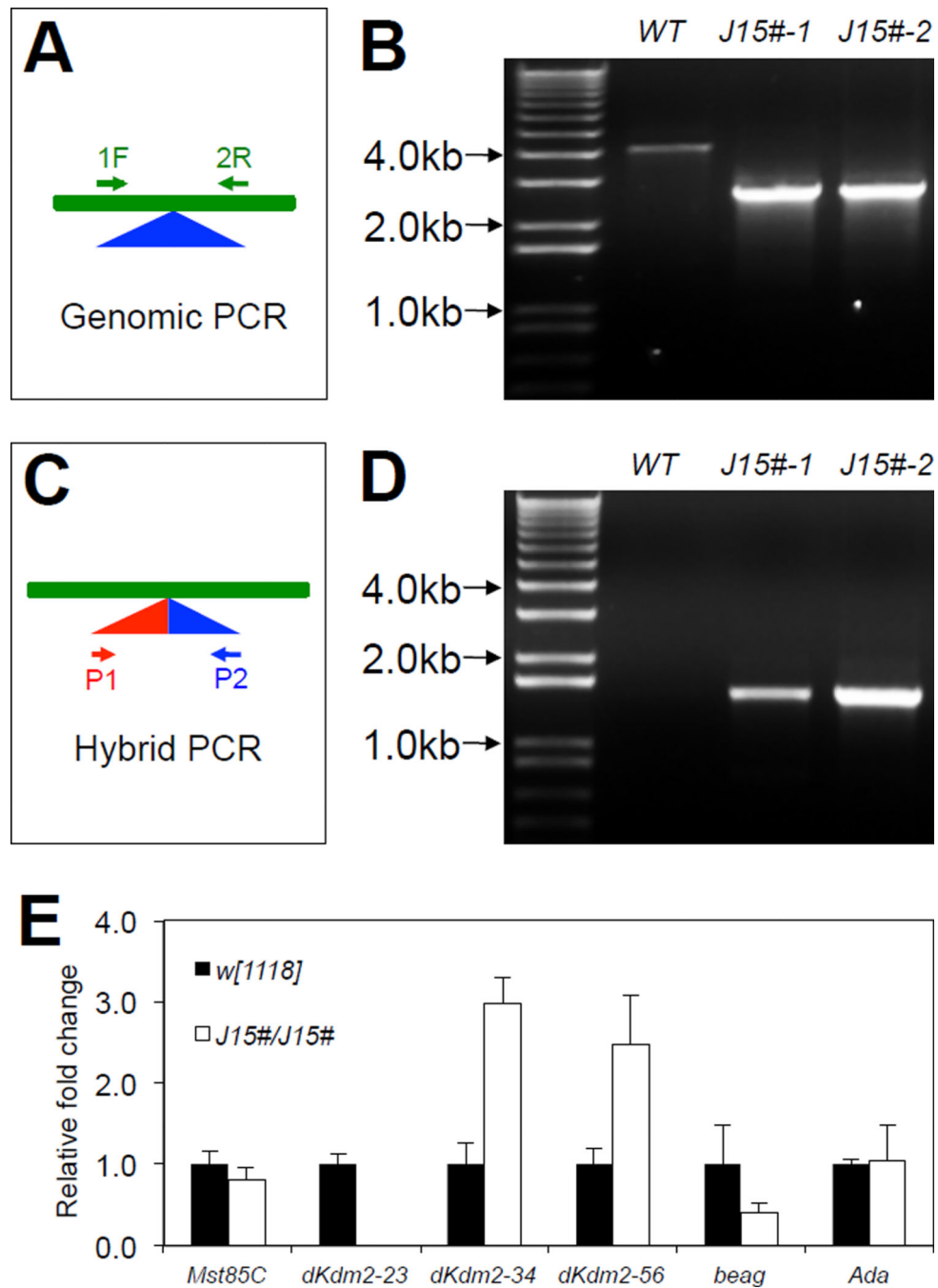
Figure 6. Validation and characterization of the *Df(3R)J15#* allele after outcrossing
Schematic representations of genomic PCR (**A**) and hybrid PCR (**C**), and the results are shown in **B** and **D**, respectively, in two independently outcrossed line *Df(3R)J15#*, designated as "*J15#-1*" and "*J15#-2*". The "*J15#-1*" line was used for subsequent analyses. (**E**) Expression of *dKdm2* and its neighboring genes assayed by qRT-PCR.
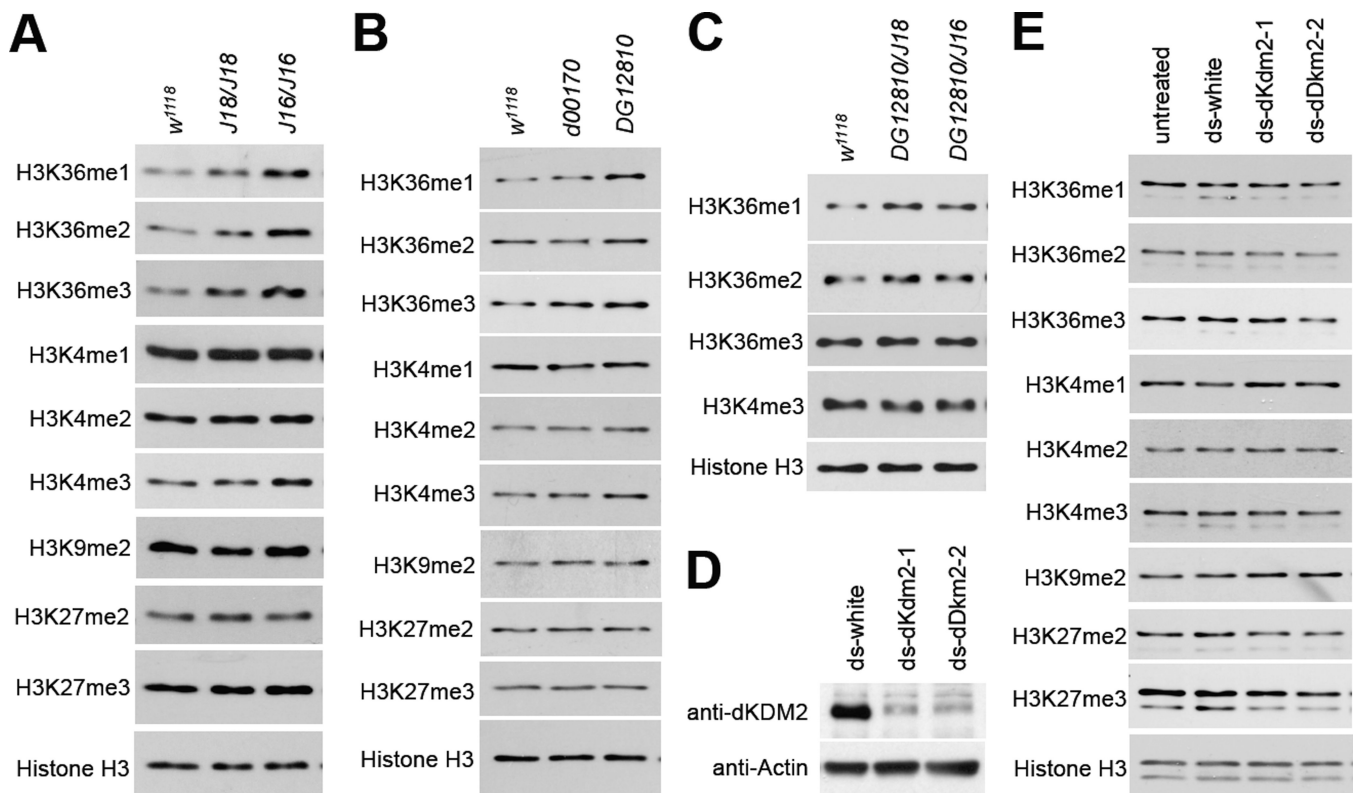
Figure 7. Effects of loss of *dKdm2* on histone lysine modifications as assayed by Western blots
(**A**) The levels of histone modifications in the *Df(3R)J16* and *Df(3R)J18* homozygous mutants during the third instar wandering stage, and *w^1118^* animals at the same stage were used as the control. Similar Western blot analysis was performed to analyze histone modification in the *dKdm2^d00170^* and *dKdm2^DG12810^* homozygous mutants (**B**), as well as the *dKdm2^DG12810^/Df(3R)J16* and *dKdm2^DG12810^/Df(3R)J18* trans heterozygous larvae (**C**). (**D**) dKDM2 protein is depleted in S2-DRSC cells using two different *dKdm2* shRNAs (*ds-dKdm2-1* and *ds-dKdm2-2*), and the effects on histone modifications were analyzed by Western blot (**E**). The dsRNA to *white* gene was used as the control. These analyses were repeated multiple times.

Table 1

Summary of the complementation genetic tests of the *dKdm2* alleles at 25°C

Complementation genetic tests of different *dKdm2* mutant alleles

	Alleles	Df(3R)JJ15	f02828	EP3093	d00170	Df(3R)JJ16	Df(3R)JJ18	DG12810	d02926	d06162	d06730	EY01336	F11.1	KG04325
	Df(3R)JJ15	lethal (L1)												
Class I	f02828	lethal (L1)	lethal (L1)											
	EP3093	viable	viable	lethal (L1)										
	d00170	viable	viable	viable	lethal (L3)									
Class II	Df(3R)JJ16	viable	viable	viable	viable	lethal (L3/P)								
	Df(3R)JJ18	viable	viable	viable	viable	Lethal (L3/P)	lethal (L3/P)							
	DG12810	viable	viable	viable	viable	viable	viable	lethal (L3/P)						
	d02926	viable	viable	viable	viable	viable	viable	viable	viable					
	d06162	viable	viable	viable	viable	viable	viable	viable	viable	viable				
Class III	d06730	viable	viable	viable	viable	viable	viable	viable	viable	viable	viable			
	EY01336	viable	viable	viable	viable	viable	viable	viable	viable	viable	viable	viable		
	F11.1	viable	viable	viable	viable	viable	viable	viable	viable	viable	viable	viable	viable	
	KG04325	viable	viable	viable	viable	viable	viable	viable	viable	viable	viable	viable	viable	viable

E: embryonic stage; L1: first instar larval stage; L3: third instar larval stage; P: pupal stage

Table 2

Summary of the complementation genetic tests of the *dKdm2* alleles after generations of outcrossing with wild-type (*w1118*) flies

Complementation genetic tests of several *dKdm2* alleles after outcrossing with wild-type (*w1118*) flies for 3 ~ 4 generations

Alleles	**Df(3R)J15**	**f02828#**	**EP3093#**	**d00170#**
f02828#	viable	lethal (L3/P)		
EP3093#	viable	viable	viable	
d00170#	viable	viable	viable	viable

L3: third instar larval stage; P: pupal stage